

# Extreme Relativistic Electron Fluxes in GPS Orbit

Nigel P. Meredith<sup>1</sup>, Thomas E. Cayton<sup>2</sup>,  
Michael D. Cayton<sup>2</sup>, and Richard B. Horne<sup>1</sup>

1. British Antarctic Survey, Cambridge, UK
2. Santa Fe, New Mexico, USA

National Space-Based Position, Navigation and Timing Advisory Board Meeting  
South Shore Harbour Resort and Conference Center, League City, Texas  
6-7<sup>th</sup> December, 2023



**British  
Antarctic Survey**

NATURAL ENVIRONMENT RESEARCH COUNCIL



# Space Weather

- Modern society is increasingly reliant on satellites for a wide variety of applications including communication, navigation, Earth observation and defence
- This ever growing infrastructure is increasingly vulnerable to the potentially damaging effects of space weather



# Space Weather

- The concern at government level in the UK is such that extreme space weather was added to the UK National Risk Register of Civil Emergencies in 2011



**National Risk Register**  
2020 edition



# Space Weather

- The concern at government level in the UK is such that extreme space weather was added to the UK National Risk Register of Civil Emergencies in 2011
- The likelihood of a reasonable worst case scenario occurring in the next year is estimated to be between 1 in 20 and 1 in 100

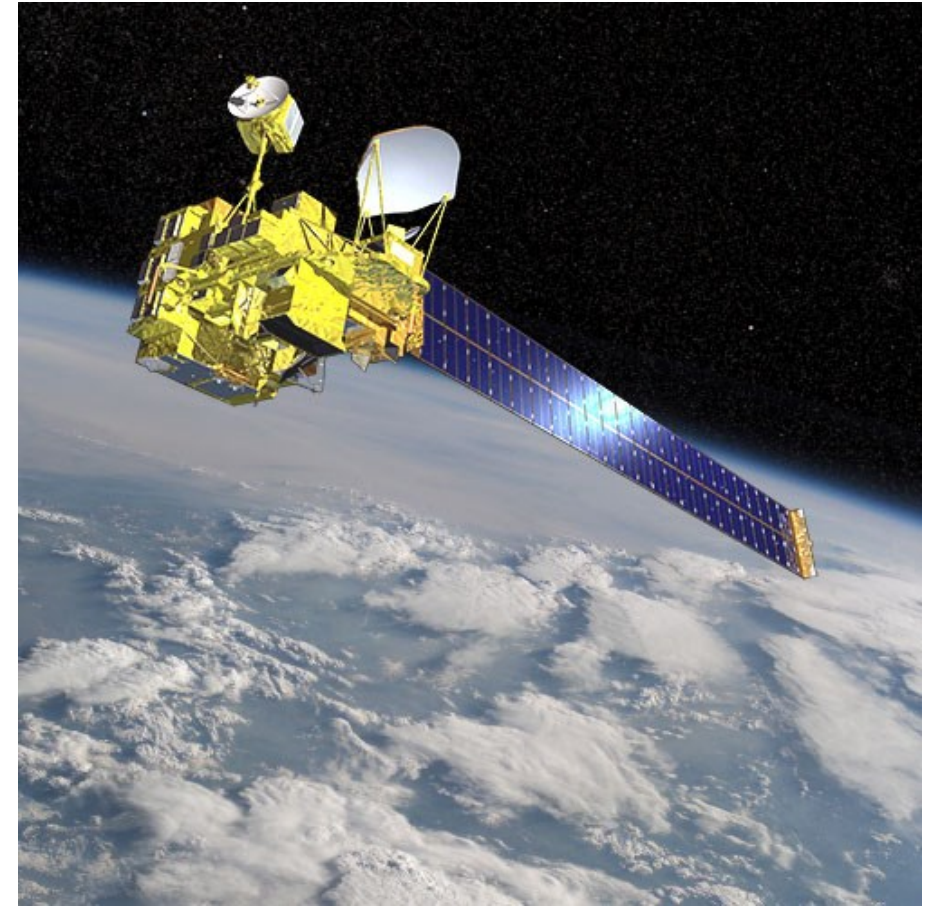


## National Risk Register 2020 edition



# Space Weather Effects on Satellites

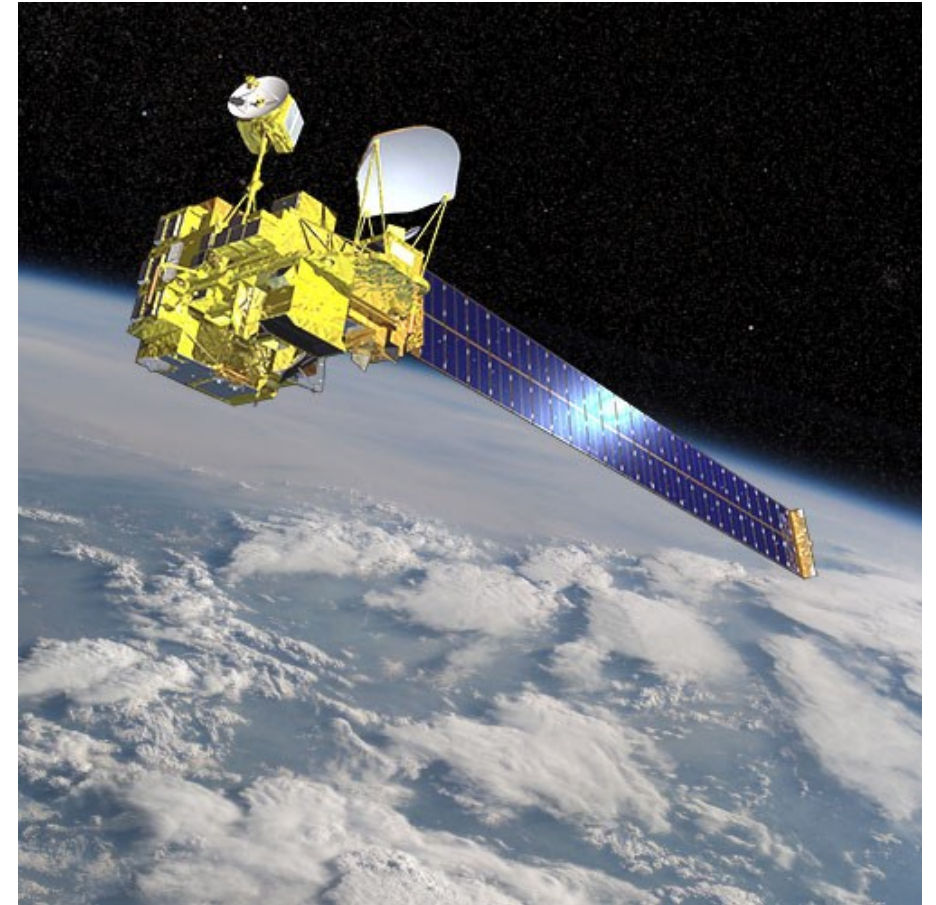
- The impacts of space weather on satellite operations range from momentary interruptions of service to total loss of capabilities when a satellite fails



Artists impression of Midori-2 satellite

# Space Weather Effects on Satellites

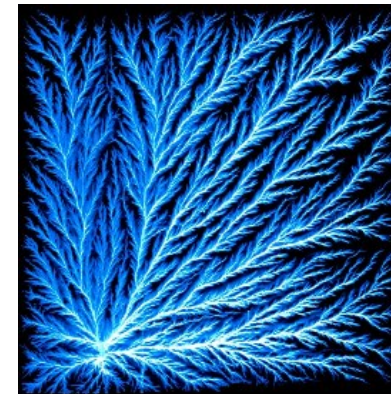
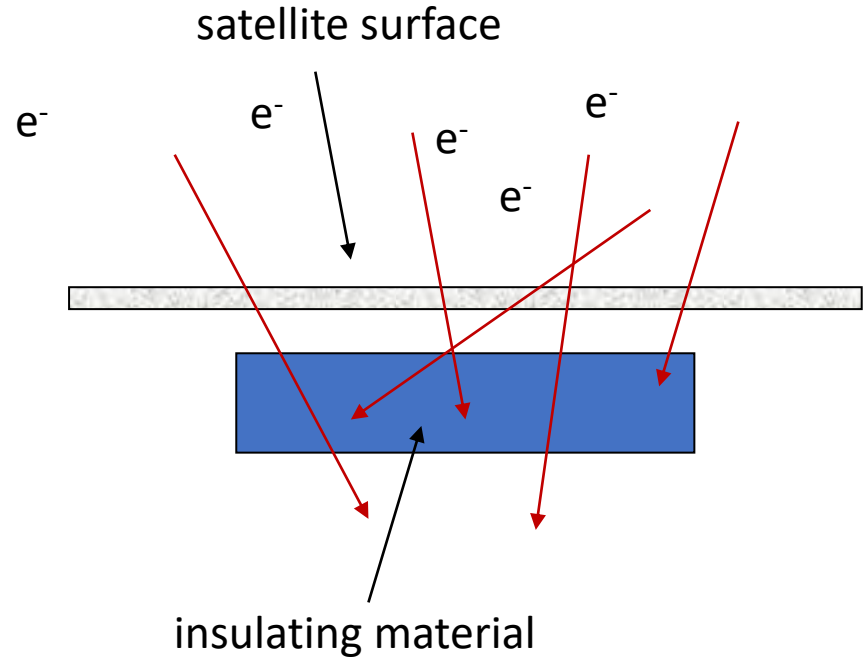
- The impacts of space weather on satellite operations range from momentary interruptions of service to total loss of capabilities when a satellite fails
- During a major storm in 2003
  - 47 satellites experienced anomalies
  - more than 10 satellites were out of action for more than 1 day
  - the US\$ 640 M Midori-2 satellite was a complete loss



Artists impression of Midori-2 satellite

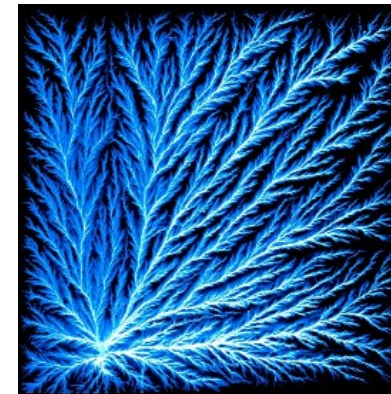
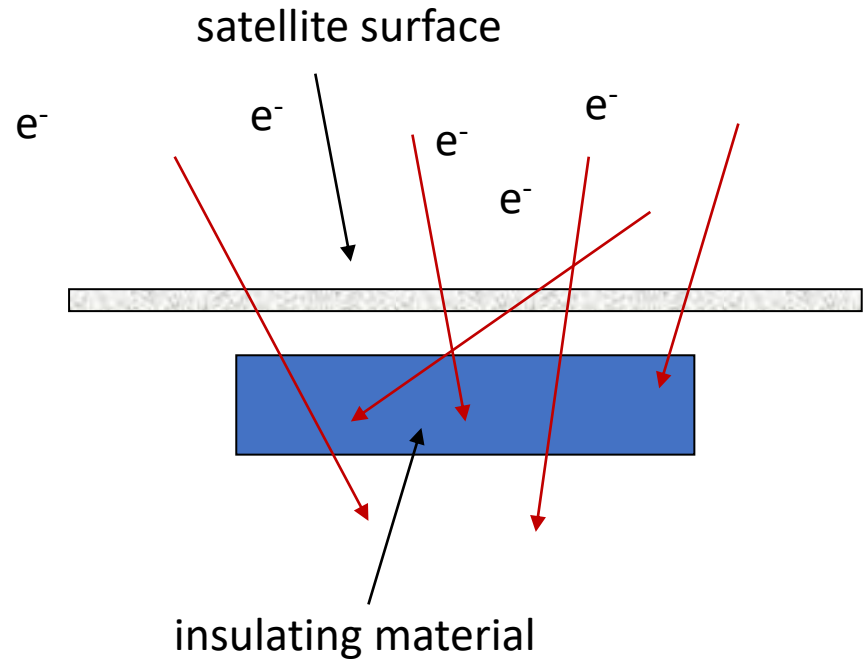
# Radiation Damage

- Relativistic electrons ( $E > 0.5 \text{ MeV}$ ) are a major source of radiation damage to satellites
- These, so called "killer electrons", can penetrate satellite surfaces and embed themselves in insulating materials



# Radiation Damage

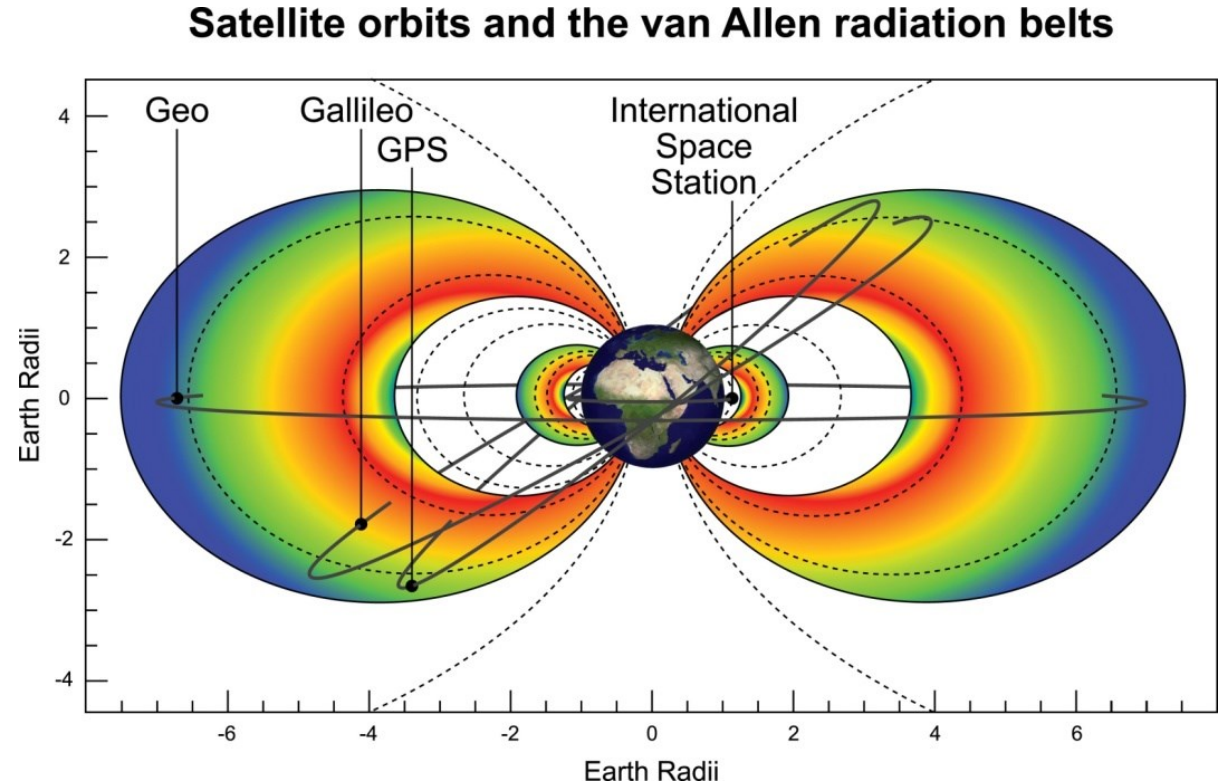
- Relativistic electrons ( $E > 0.5 \text{ MeV}$ ) are a major source of radiation damage to satellites
- These, so called "killer electrons", can penetrate satellite surfaces and embed themselves in insulating materials
- The charge can accumulate over time resulting in the build up of high electric fields which may eventually exceed breakdown levels
- The subsequent discharge can damage components and even destroy a satellite





# Earth's Radiation Belts

- Our critical infrastructure extends to 6.6 Earth radii
- Over 6700 operational satellites in Earth orbit including
  - 5900 in low Earth orbit
  - 140 in medium Earth orbit
  - 580 in geostationary orbit
- Most are exposed to relativistic electrons ( $E > 500$  keV) in the Earth's radiation belts



# GNSS Satellites

- GNSS satellites such as the US GPS satellites and the European Galileo navigation system operate in MEO at altitudes between 19,000 and 24,000 km
- GNSS enabled devices are used all over the world for navigation, positioning, tracking, mapping and timing

# GNSS Satellites

- GNSS satellites such as the US GPS satellites and the European Galileo navigation system operate in MEO at altitudes between 19,000 and 24,000 km
- GNSS enabled devices are used all over the world for navigation, positioning, tracking, mapping and timing
- It is, therefore, important to have a comprehensive understanding of the environment encountered by satellites in GNSS-type orbits and, in particular, knowledge of the likely extremes of this environment

# Objective

- The objective of this study is to calculate the 1 in 10 and 1 in 100 year relativistic electron fluxes throughout the Earth's outer radiation belt in GPS orbit

# Extreme Relativistic Electron Fluxes

- The data used in this study were collected by the Burst Detector Dosimeter IIR (BDD-IIR) on board the GPS satellite NS41
- The satellite was launched on 10<sup>th</sup> November 2000 and operated in a circular orbit at an altitude of 20,200 km with an inclination of 55° and a period of 12 hours
- It crossed the magnetic equator around  $L = 4.2$  and sampled higher L shells at higher latitudes
- We use data from 10<sup>th</sup> December 2000 to 25<sup>th</sup> July 2020

## GPS Block IIR

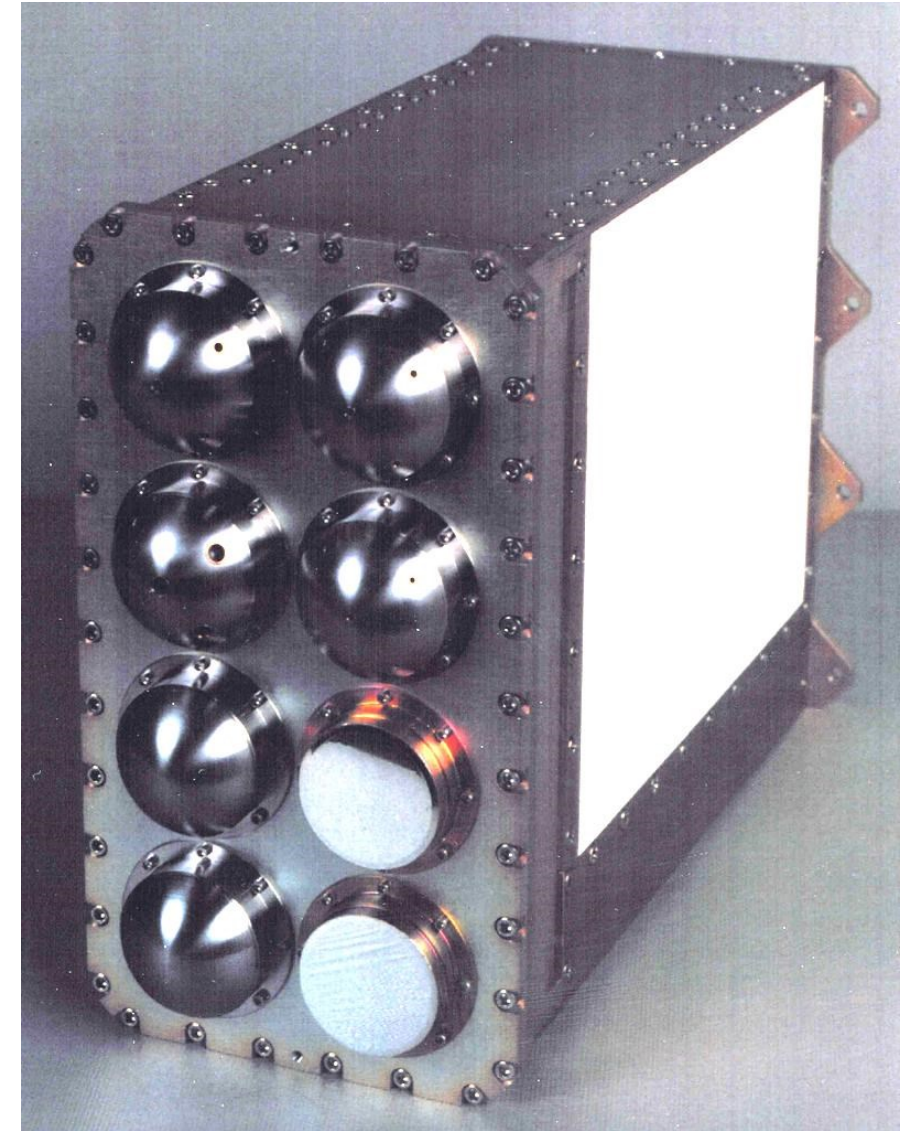


Credit: Lockheed Martin

Orbital Parameters	
Altitude:	20,200 km
Inclination:	55°
Period:	12 h

# BDD-IIR

- BDD-IIR is a multi-purpose silicon detector system
- It features 8 individual channels of a "shield/filter/sensor" design
- Absorbers in front of the sensors determine the energy thresholds for measuring the incident particle fluxes

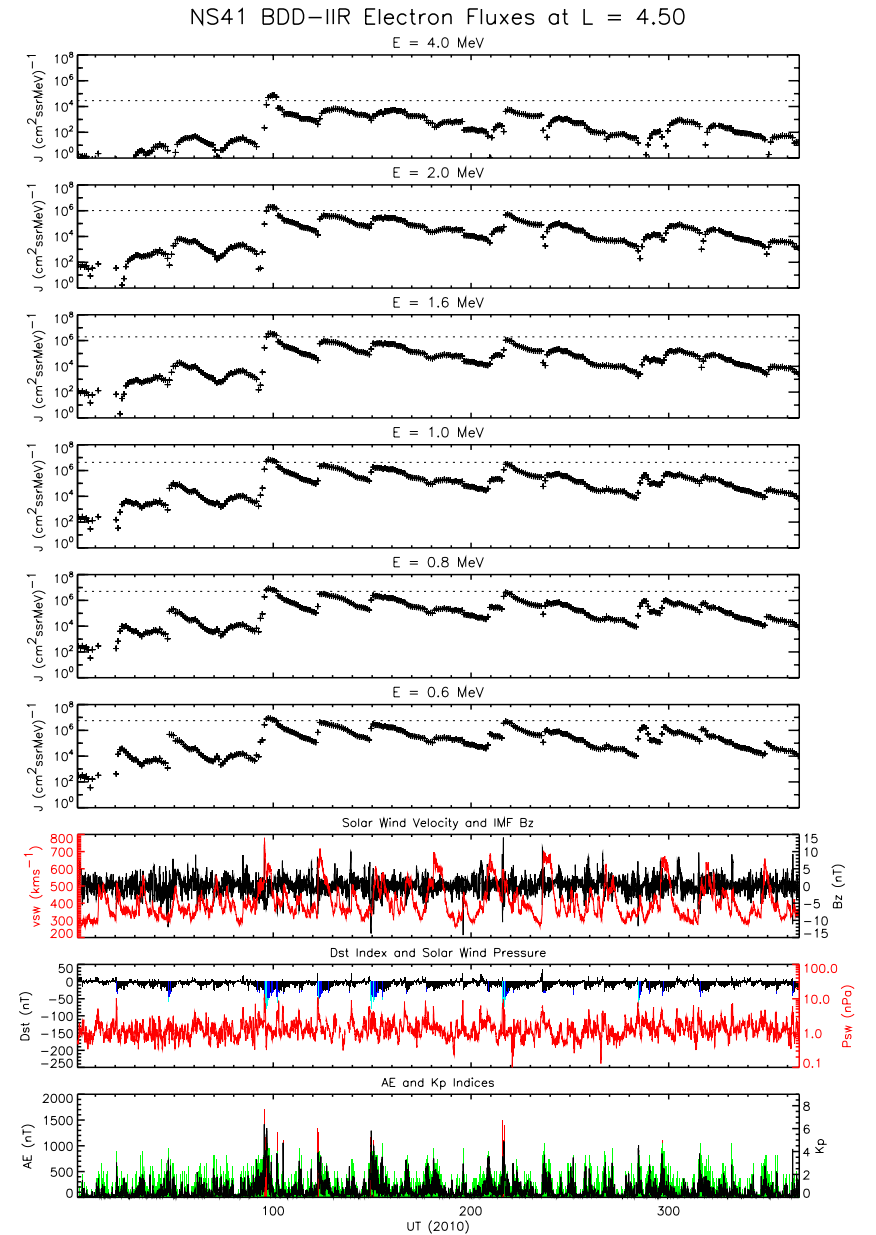


# Data Processing

- Differential fluxes at 10 energies in the range  $0.6 \leq E \leq 8$  MeV were written into separate files for each crossing of 12 equally spaced L shells in the range  $4.25 \leq L \leq 7.00$
- Daily averaged fluxes were then computed for each energy and L shell
- Here L is the McIlwain L value computed using the IGRF internal field and the Olson-Pfitzer quiet time external field

# Annual Plots

- To inspect the data we produced annual summary plots
- This figure shows the annual summary plot at  $L = 4.5$  for 2010 for six representative energies
- At each energy the fluxes are characterised by relatively rapid increases followed by gradual decays lasting many days

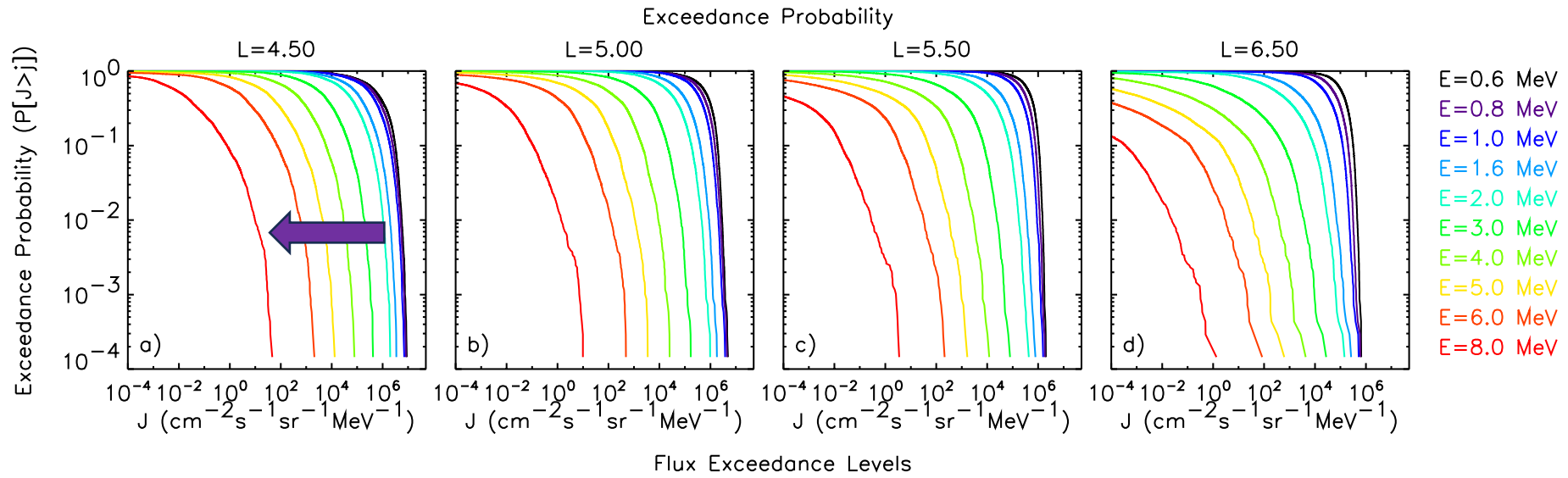




# Exceedance Probabilities and Flux Exceedance Levels

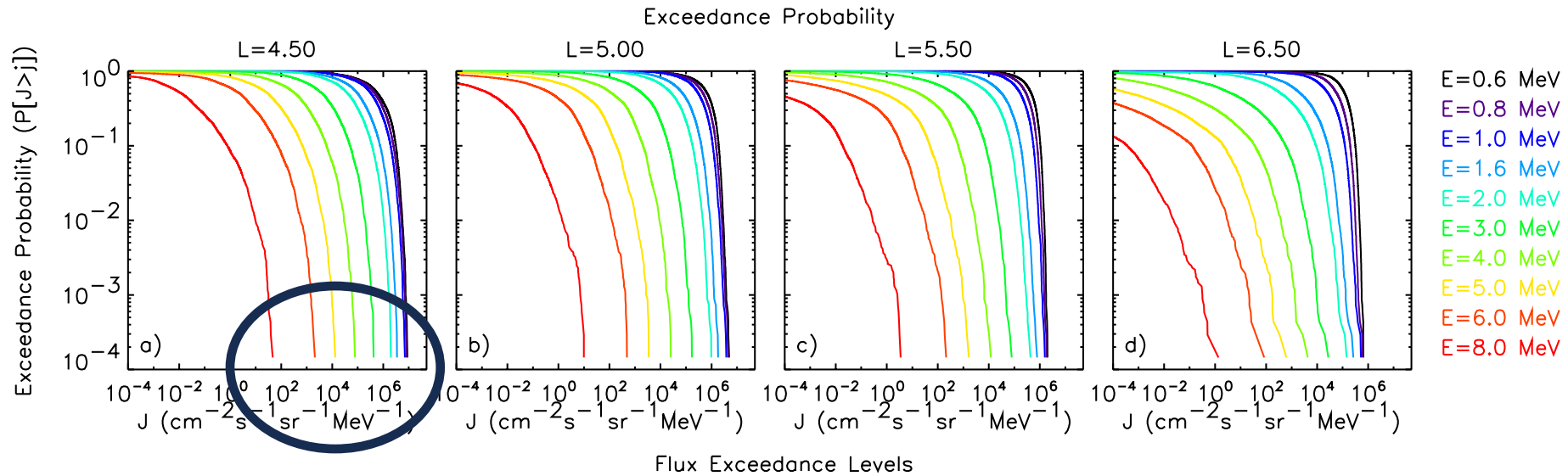
- We plotted the exceedance probabilities as a function of electron flux for each energy and for each value of L

# Statistical Analysis of NS41 BDD-IIR Fluxes



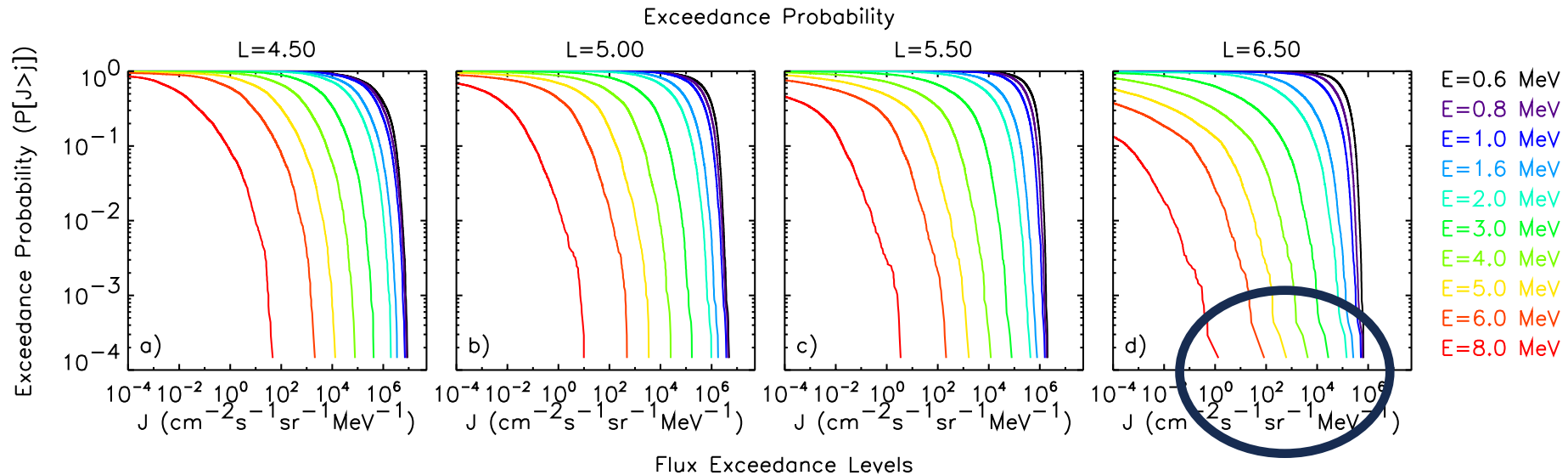
- The observed flux for any given exceedance probability decreases with increasing energy

# Statistical Analysis of NS41 BDD-IIR Fluxes



- The observed flux for any given exceedance probability decreases with increasing energy
- In the heart of the outer radiation belt, at  $L = 4.5$ , the largest observed fluxes cover over 5 orders of magnitude ranging from  $8.9 \times 10^6 \text{ cm}^{-2}\text{s}^{-1}\text{sr}^{-1}\text{MeV}^{-1}$  at  $E = 0.6 \text{ MeV}$  to  $46 \text{ cm}^{-2}\text{s}^{-1}\text{sr}^{-1}\text{MeV}^{-1}$  at  $E = 8.0 \text{ MeV}$

# Statistical Analysis of NS41 BDD-IIR Fluxes



- The observed flux for any given exceedance probability decreases with increasing energy
- In the heart of the outer radiation belt, at  $L = 4.5$ , the largest observed fluxes cover over 5 orders of magnitude ranging from  $8.9 \times 10^6 \text{ cm}^{-2}\text{s}^{-1}\text{sr}^{-1}\text{MeV}^{-1}$  at  $E = 0.6 \text{ MeV}$  to  $46 \text{ cm}^{-2}\text{s}^{-1}\text{sr}^{-1}\text{MeV}^{-1}$  at  $E = 8.0 \text{ MeV}$
- At  $L = 6.5$ , on field lines that map to geostationary orbit, the largest fluxes are factors of 13 and 34 lower than those at  $L = 4.5$  at  $E = 0.6$  and  $8.0 \text{ MeV}$  respectively

# Extreme Value Analysis

- The main objective of this study is to determine the 1 in 10 and 1 in 100 year daily average electron flux for specified energies and L shells
- Since daily averages are available and to compare with previous studies we use the exceedances over a high threshold method
- For this approach the appropriate distribution function is the Generalised Pareto Distribution (GPD)

# Extreme Value Analysis

- Based on experience analysing other satellite datasets we set the threshold at the 1% exceedance level
- We declustered the data to avoid counting individual events more than once by assuming a cluster to be active until the three consecutive daily averages fall below our chosen threshold
- We then fit the GPD to the cluster maxima for each specified energy and L shell

# Generalised Pareto Distribution

- The GPD may be written in the form

$$G(x-u) = 1 - (1 + \xi(x-u)/\sigma)^{-1/\xi}$$

where:  $x$  are the cluster maxima above the chosen threshold  $u$

$\xi$  is the shape parameter which controls the behaviour of the tail

$\sigma$  is the scale parameter which determines the dispersion or spread of the distribution

- We fit the GPD to the tail of the distribution using maximum likelihood estimation

# Determination of the 1 in N Year Event

- The flux that is exceeded on average once every N years can be expressed in terms of the fitted parameters  $\sigma$  and  $\xi$  as:

$$x_N = u + (\sigma/\xi)(Nn_d n_c/n_{\text{tot}})^\xi - 1))$$

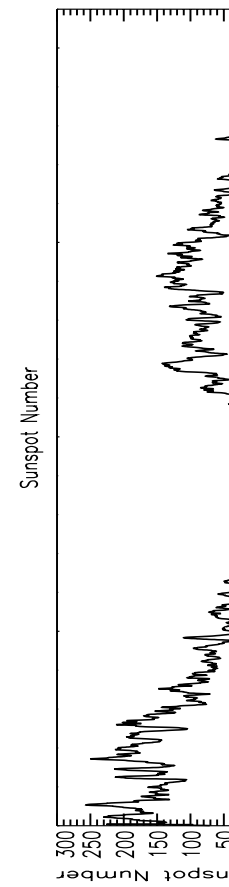
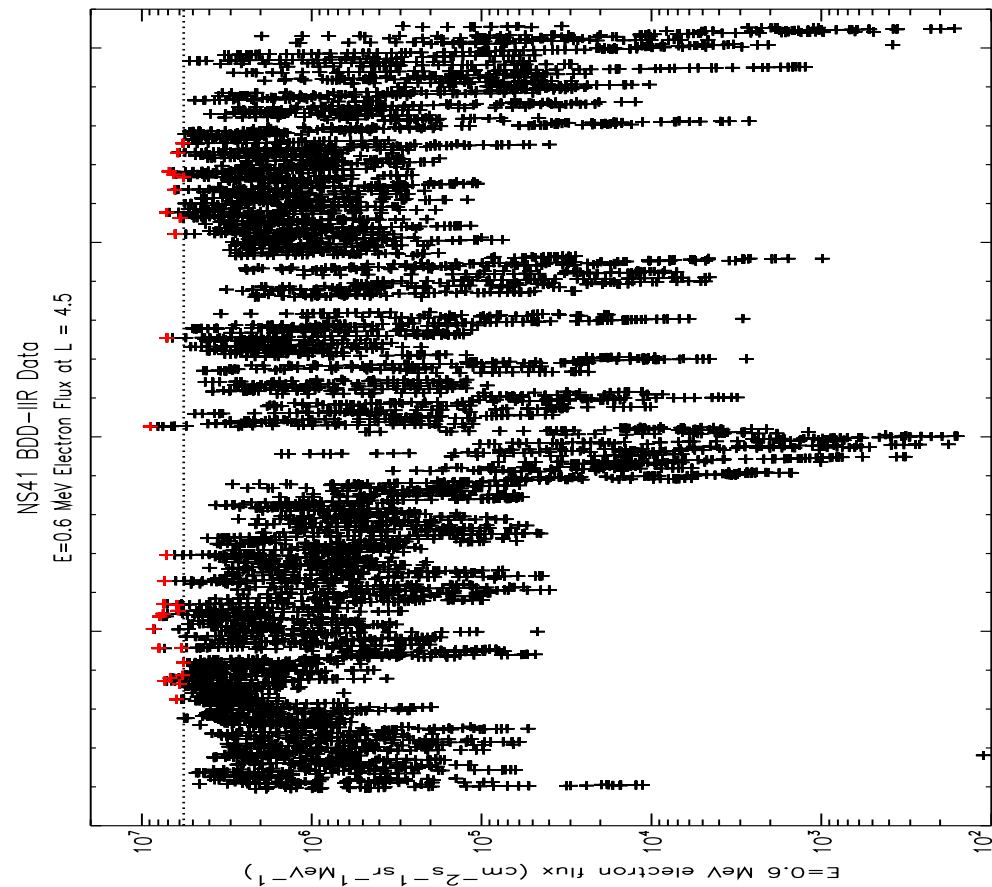
where  $n_d$  is the number of data points in a given year,  $n_c$  is the number of cluster maxima and  $n_{\text{tot}}$  is the total number of data points

- A plot of  $x_N$  against N is known as a return level plot



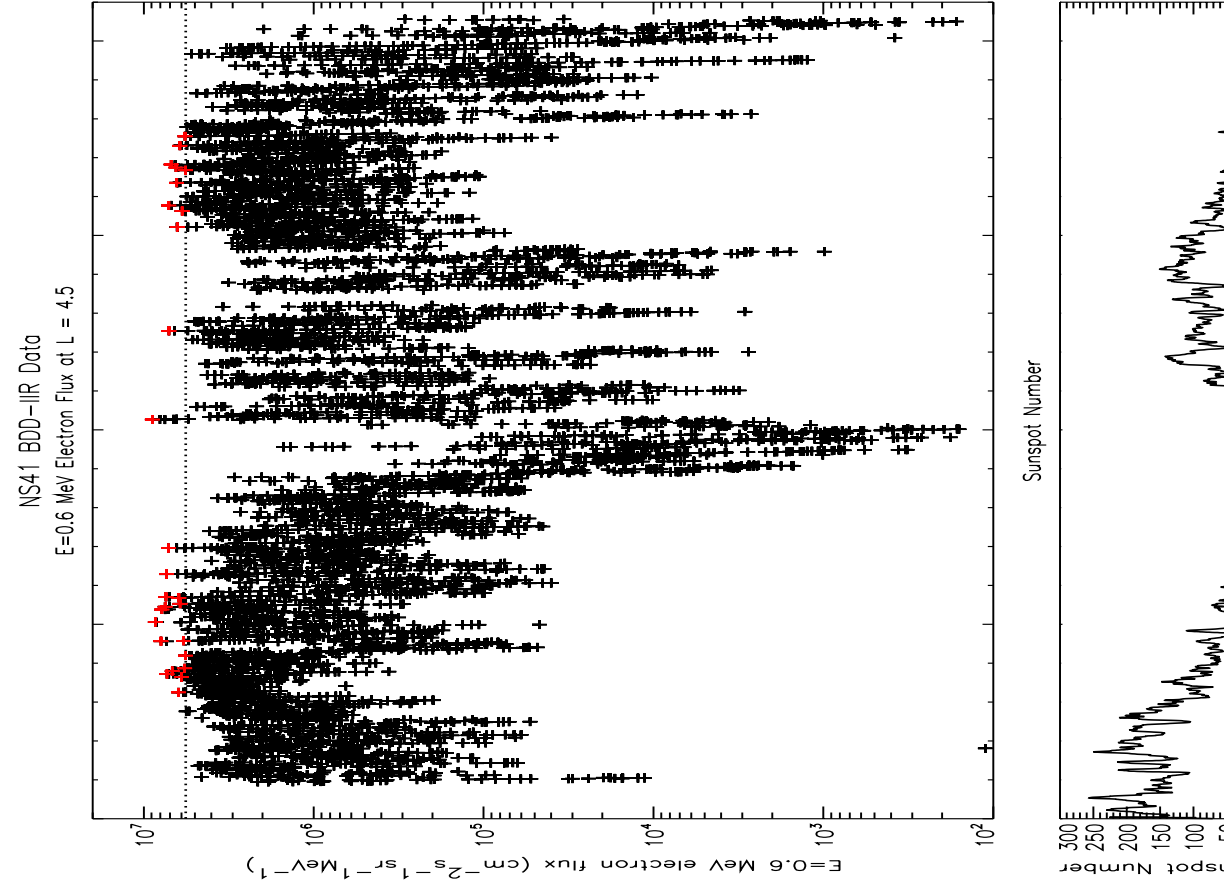
# E = 0.6 MeV Electrons at L = 4.5

- This figure shows the E = 0.6 MeV daily average electron flux for the entire mission



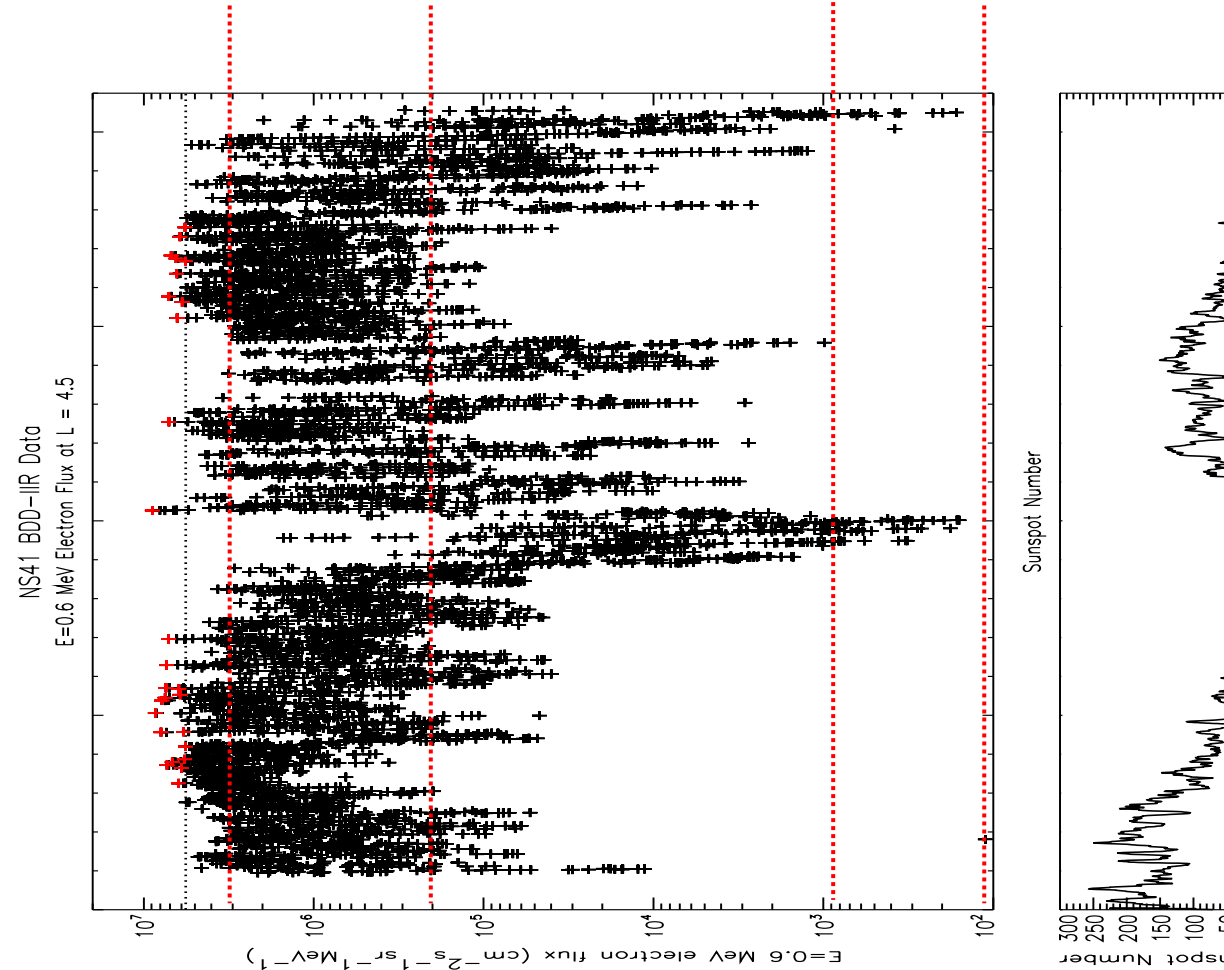
# $E = 0.6$ MeV Electrons at $L = 4.5$

- This figure shows the  $E = 0.6$  MeV daily average electron flux for the entire mission
- The 1% exceedance level, chosen as the threshold for the analysis, is shown as the dotted line and the cluster maxima are coded red



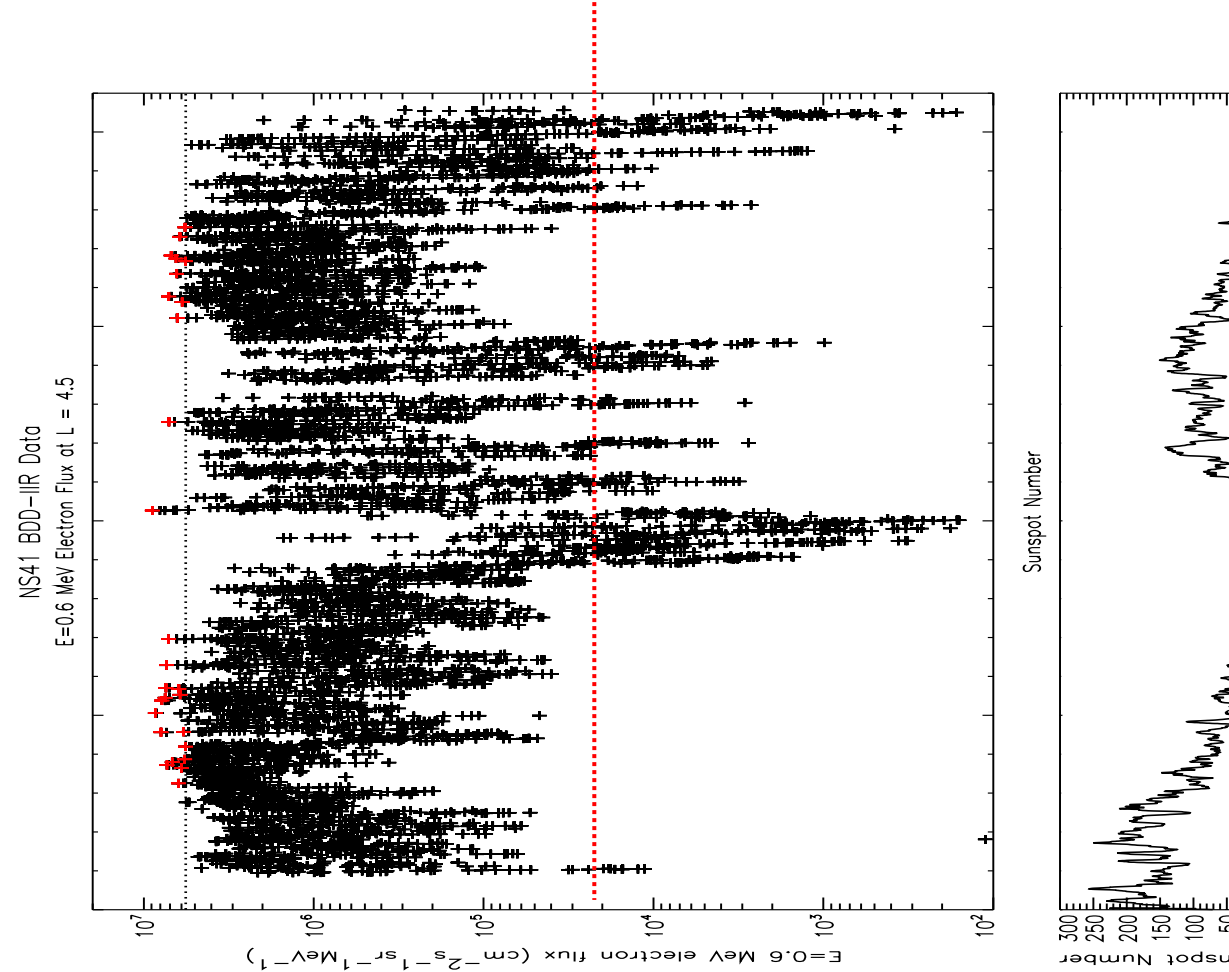
# E = 0.6 MeV Electrons at L = 4.5

- This figure shows the E = 0.6 MeV daily average electron flux for the entire mission
- The 1% exceedance level, chosen as the threshold for the analysis, is shown as the dotted line and the cluster maxima are coded red
- The largest fluxes of E = 0.6 MeV electrons at L = 4.5 are largely seen from 2003-2008 and 2015-2018, during the declining phases of solar cycles 23 and 24



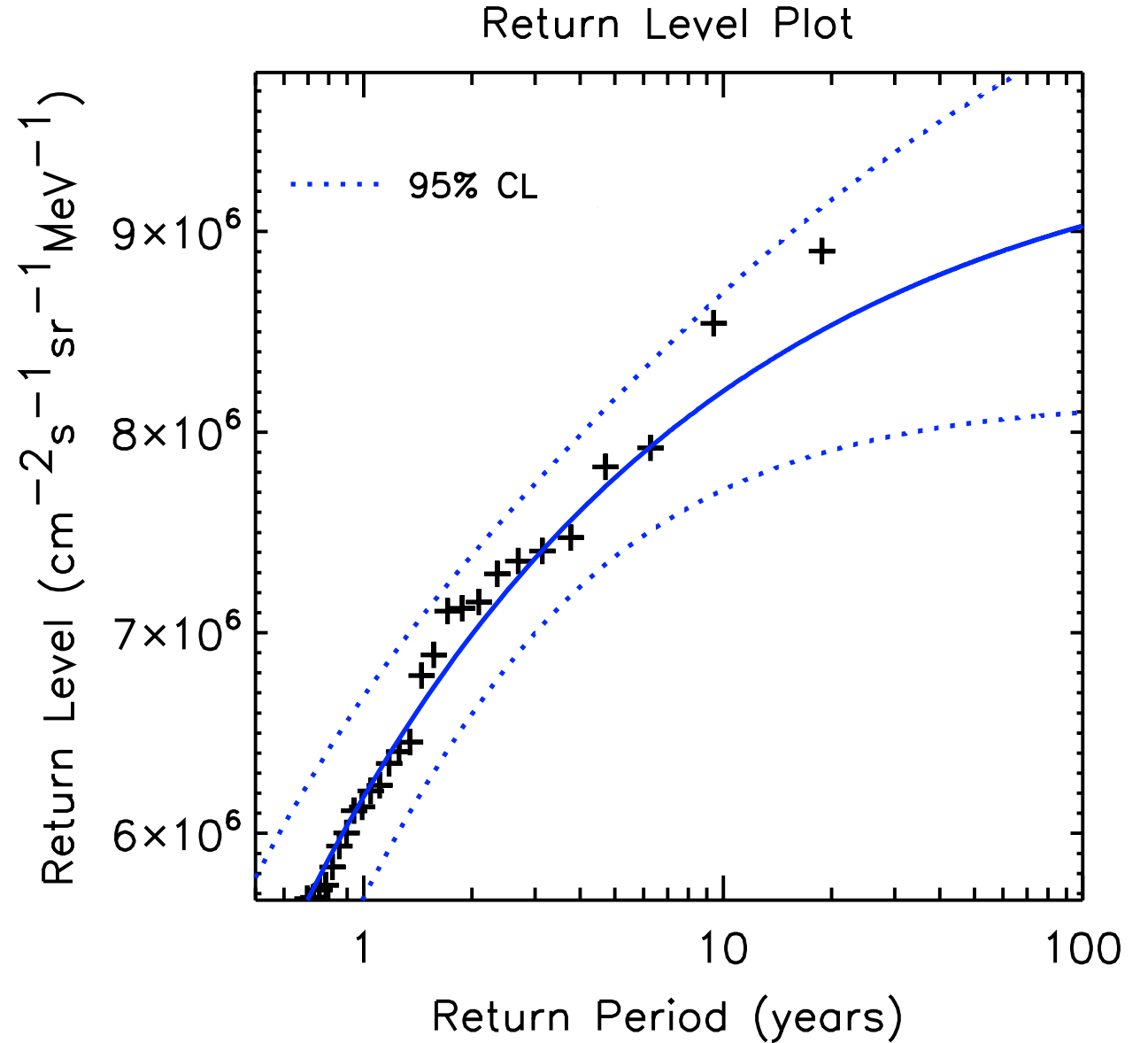
# E = 0.6 MeV Electrons at L = 4.5

- This figure shows the E = 0.6 MeV daily average electron flux for the entire mission
- The 1% exceedance level, chosen as the threshold for the analysis, is shown as the dotted line and the cluster maxima are coded red
- However, the largest event occurred near solar minimum – showing that an extreme event can occur at any time in the solar cycle



# Return Level Plot

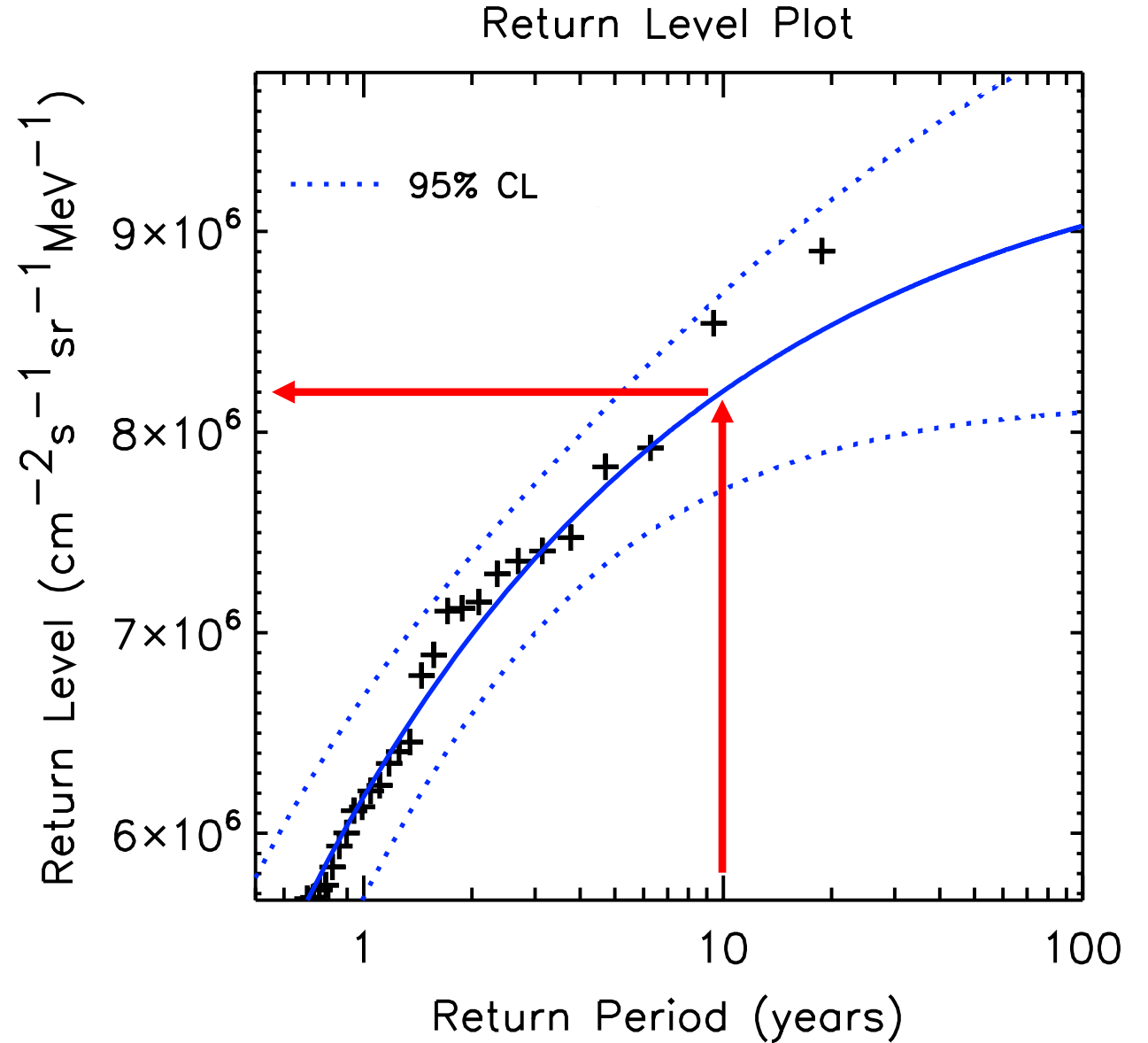
This figure shows the return level plot for 0.6 MeV electrons at L = 4.5



# Return Level Plot

This figure shows the return level plot for 0.6 MeV electrons at L = 4.5

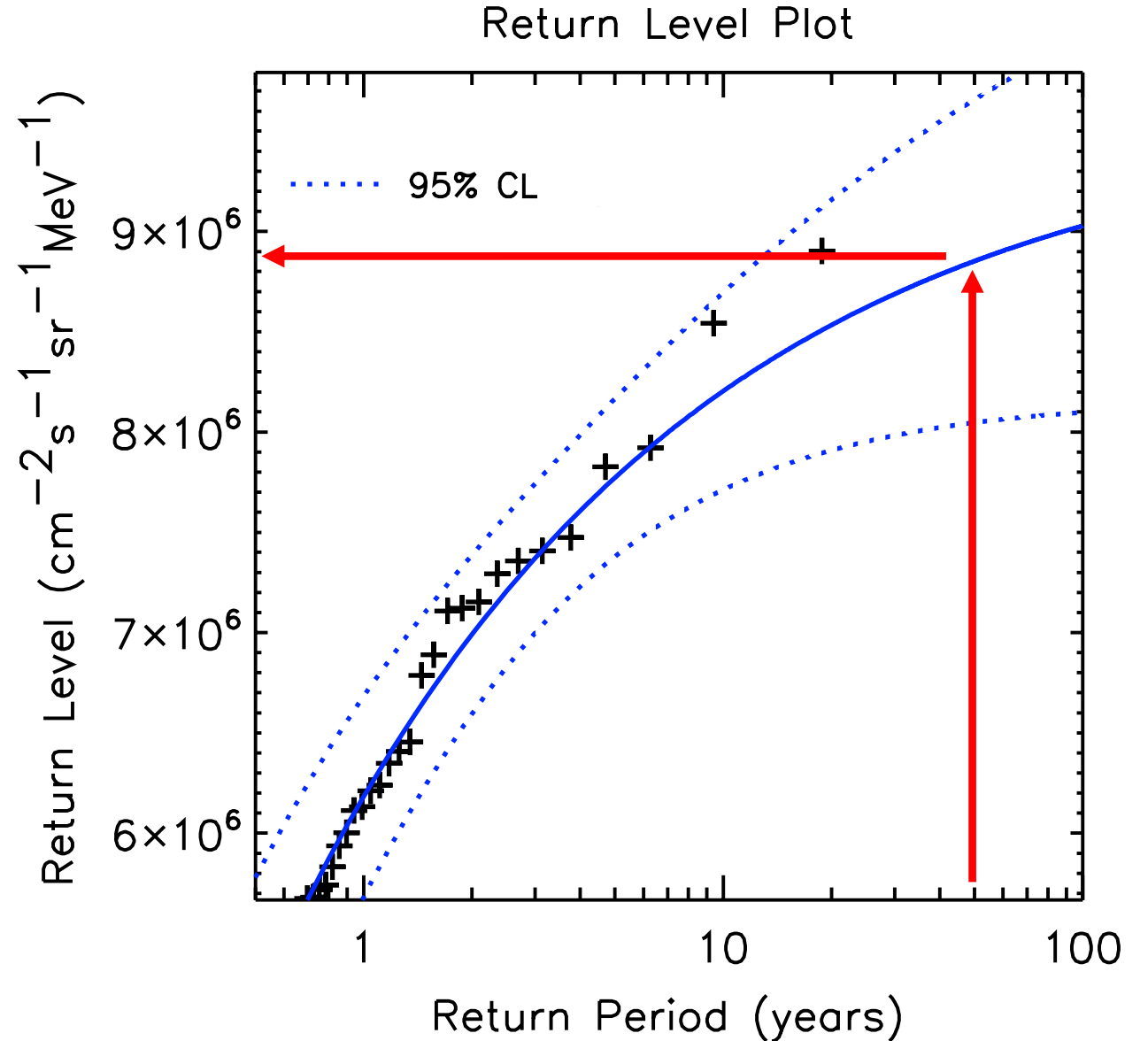
- 1 in 10 year daily-average flux
  - $8.2 \times 10^6 \text{ cm}^{-2} \text{ s}^{-1} \text{ sr}^{-1} \text{ MeV}^{-1}$



# Return Level Plot

This figure shows the return level plot for 0.6 MeV electrons at L = 4.5

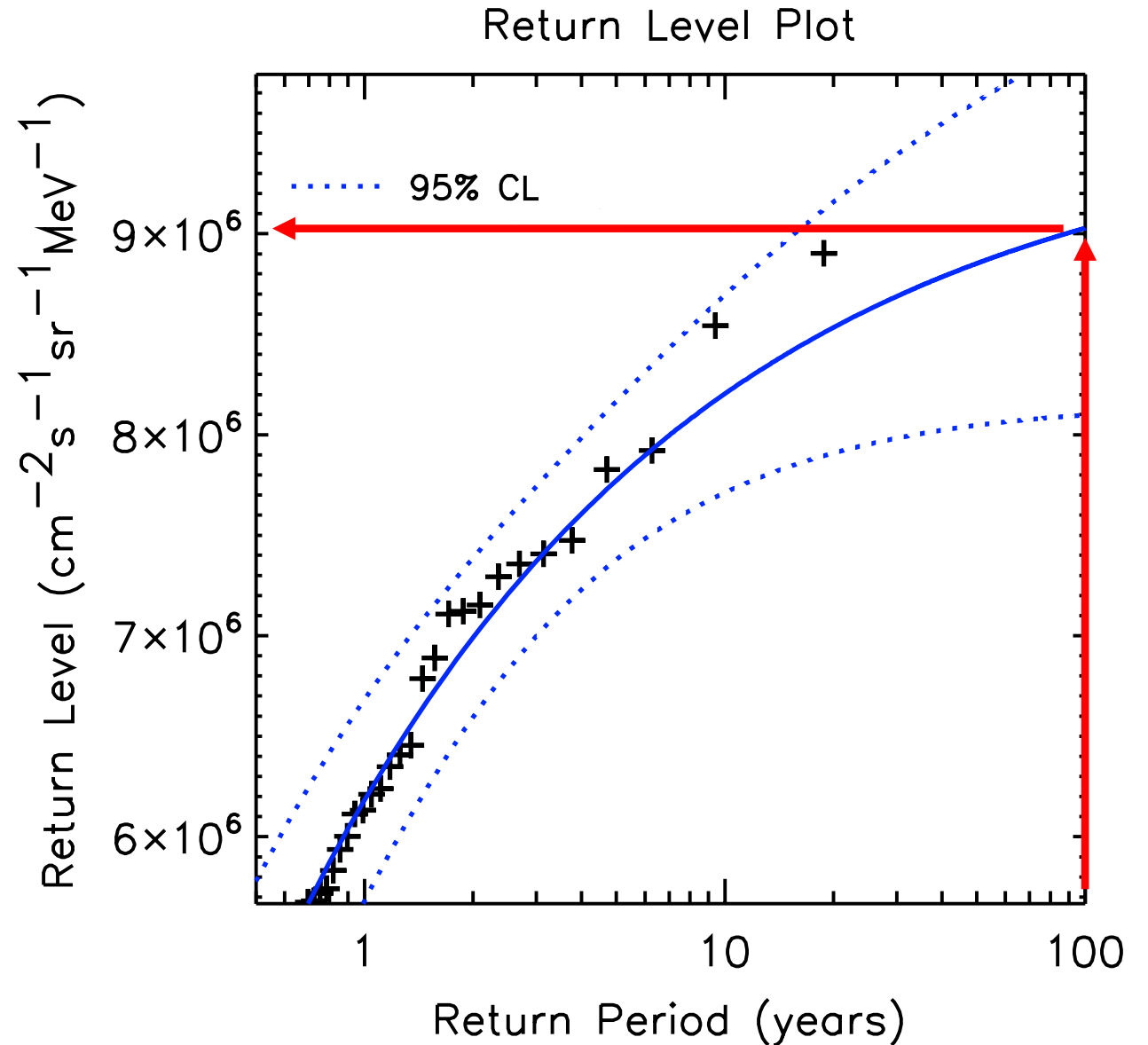
- 1 in 10 year daily-average flux
  - $8.2 \times 10^6 \text{ cm}^{-2} \text{ s}^{-1} \text{ sr}^{-1} \text{ MeV}^{-1}$
- 1 in 50 year daily-average flux
  - $8.9 \times 10^6 \text{ cm}^{-2} \text{ s}^{-1} \text{ sr}^{-1} \text{ MeV}^{-1}$



# Return Level Plot

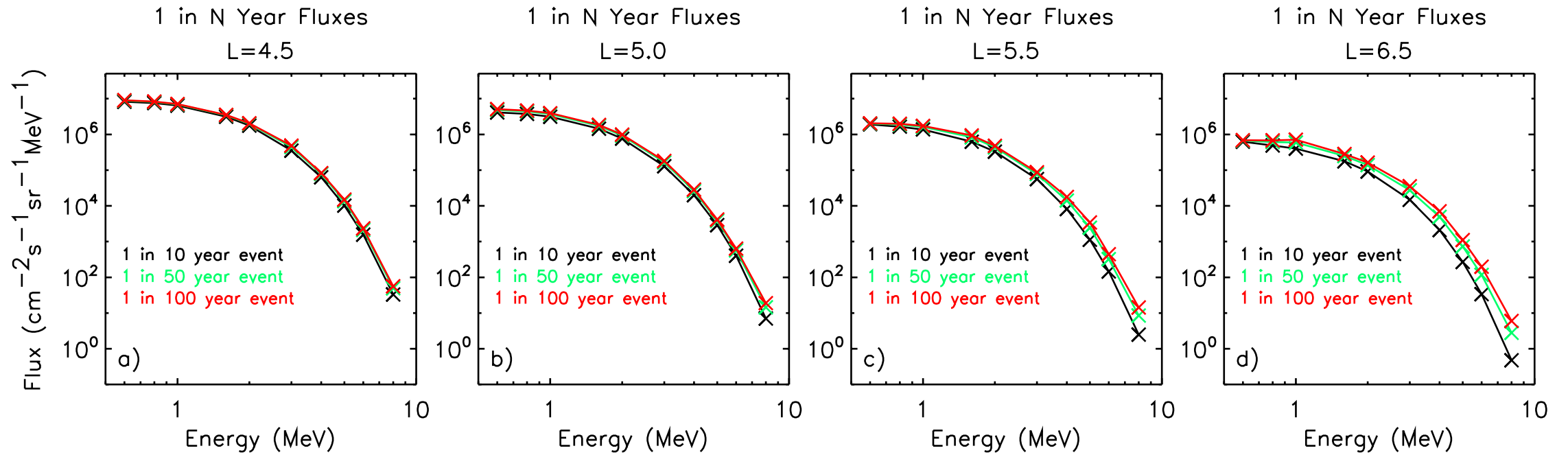
This figure shows the return level plot for 0.6 MeV electrons at L = 4.5

- 1 in 10 year daily-average flux
  - $8.2 \times 10^6 \text{ cm}^{-2} \text{ s}^{-1} \text{ sr}^{-1} \text{ MeV}^{-1}$
- 1 in 50 year daily-average flux
  - $8.9 \times 10^6 \text{ cm}^{-2} \text{ s}^{-1} \text{ sr}^{-1} \text{ MeV}^{-1}$
- 1 in 100 year daily-average flux
  - $9.0 \times 10^6 \text{ cm}^{-2} \text{ s}^{-1} \text{ sr}^{-1} \text{ MeV}^{-1}$



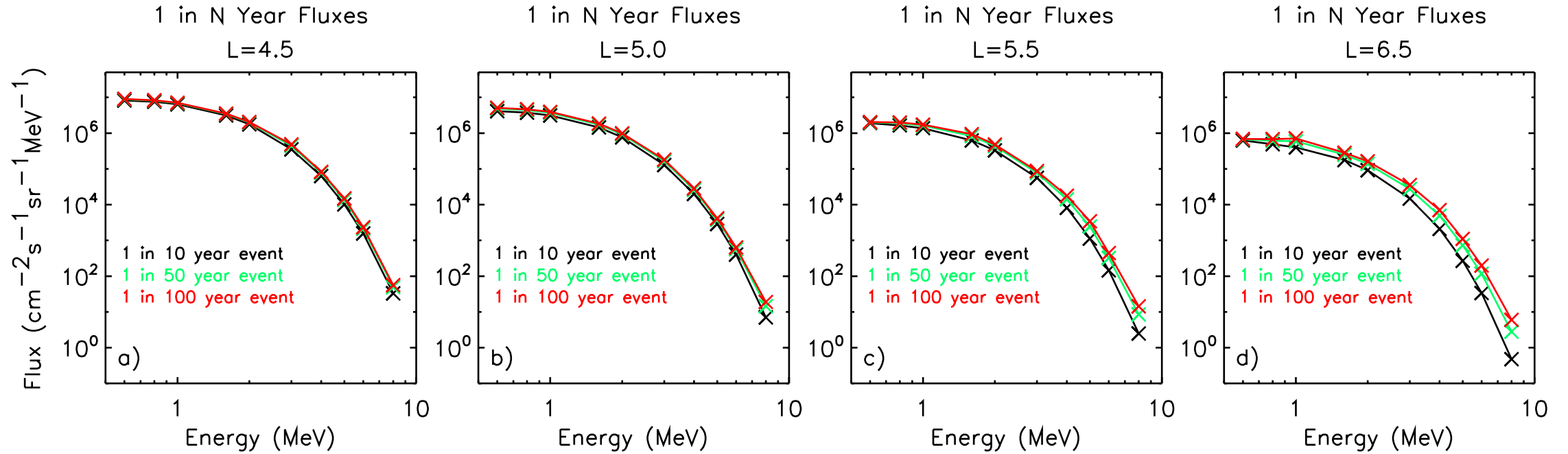


# 1 in N Year Fluxes



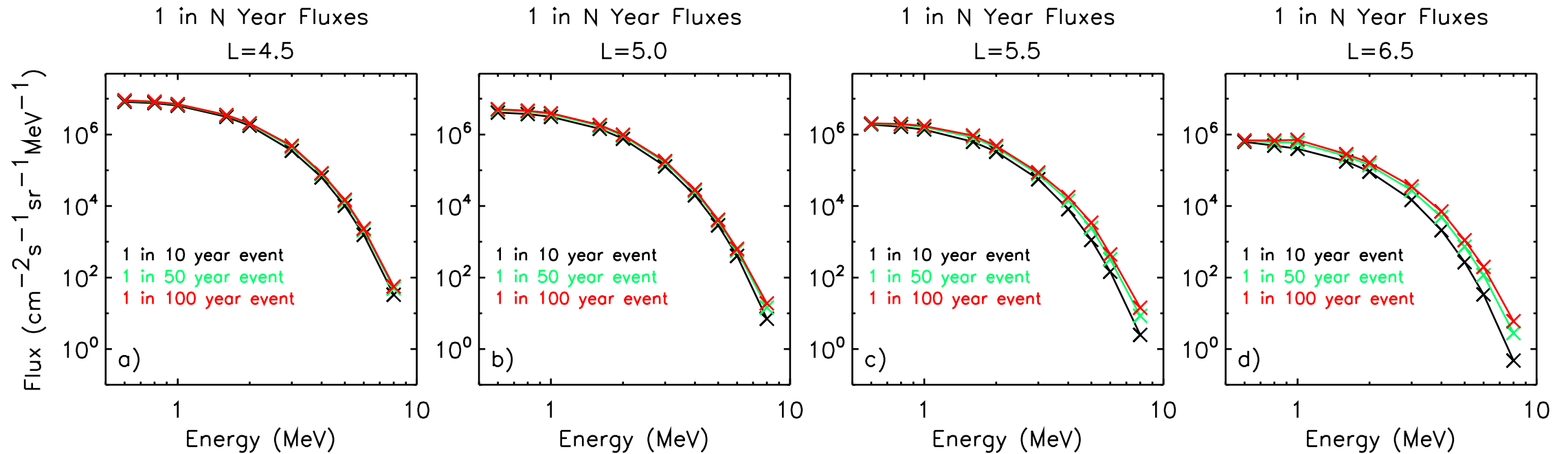
- The 1 in N Year fluxes decrease with increasing energy

# 1 in N Year Fluxes



- The 1 in N Year fluxes decrease with increasing energy
- At  $L = 4.5$  there is very little difference between the 1 in 10 and 1 in 100 year events

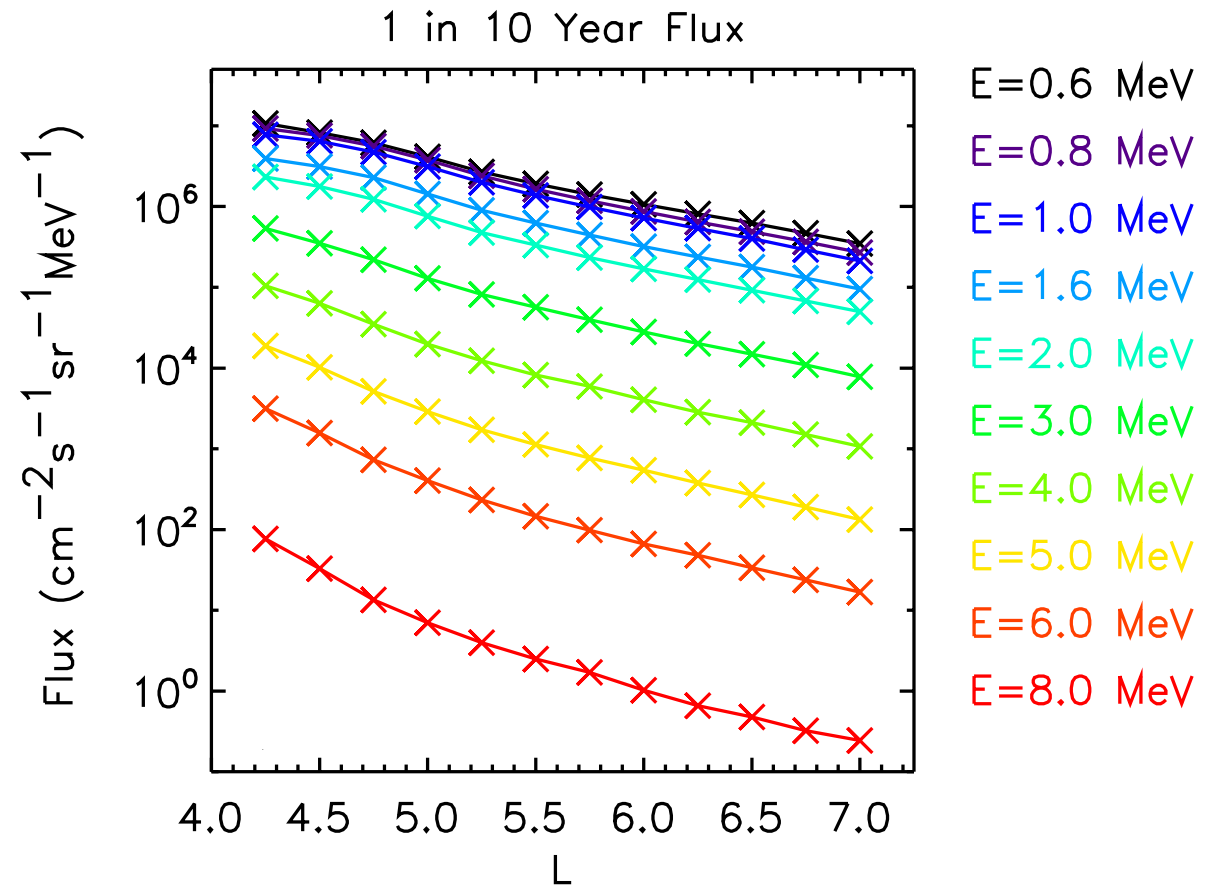
# 1 in N Year Fluxes



- The 1 in N Year fluxes decrease with increasing energy
- At  $L = 4.5$  there is very little difference between the 1 in 10 and 1 in 100 year events
- Further out there is an increasing tendency for a larger difference between the 1 in 10 and 1 in 100 year events, particularly at higher energies

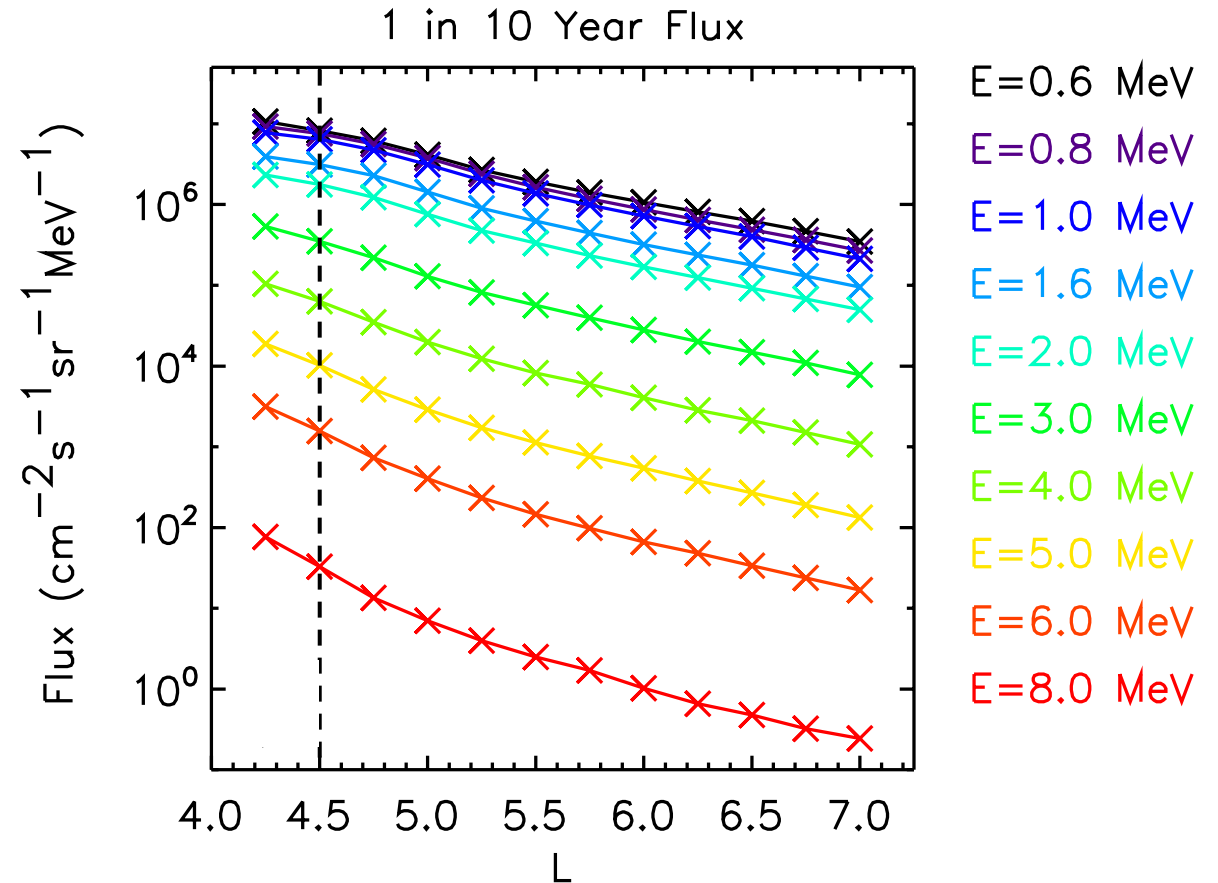
# 1 in 10 Year Fluxes as a function of L and Energy

- We can summarise the 1 in N year electron fluxes as a function of L for the different energies



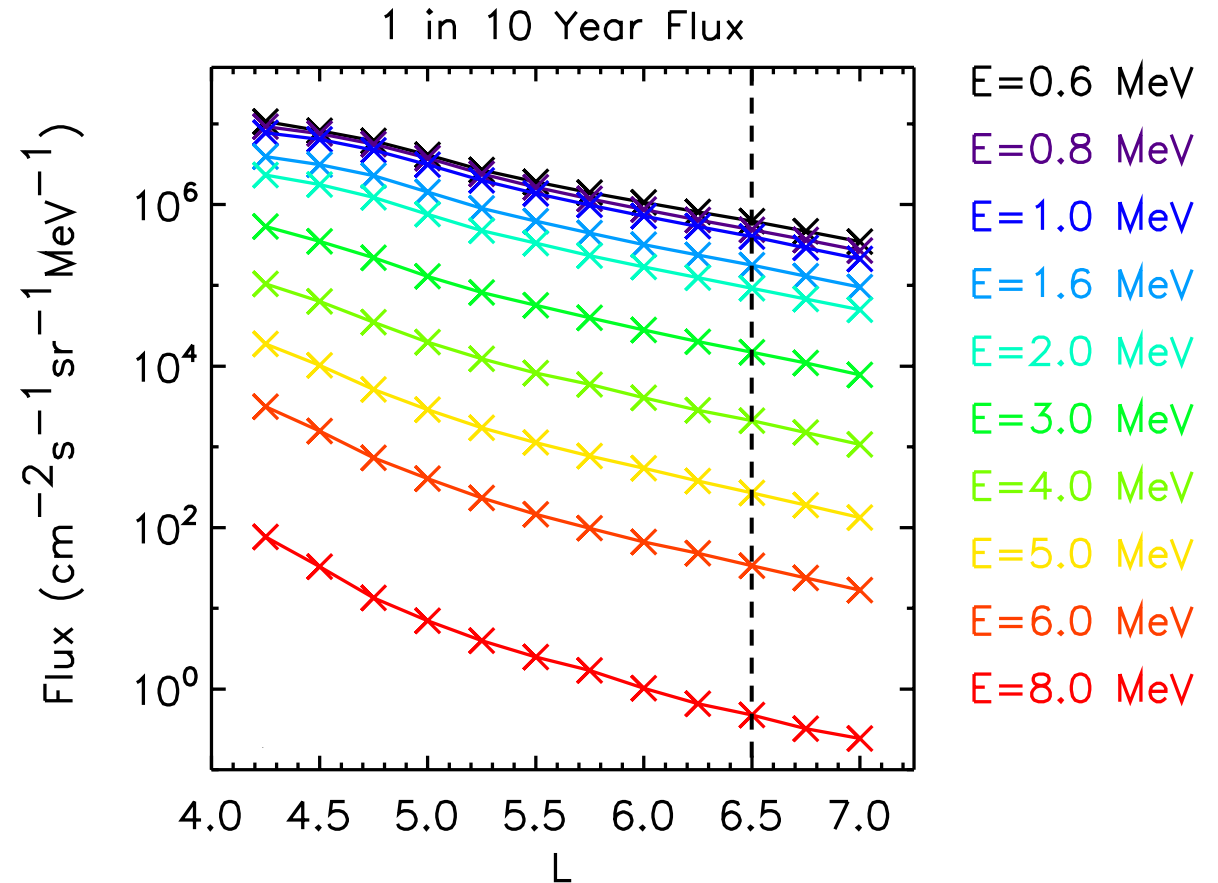
# 1 in 10 Year Fluxes as a function of L and Energy

- We can summarise the 1 in N year electron fluxes as a function of L for the different energies
- The 1 in 10 year flux at L = 4.5 ranges from  $8.2 \times 10^6 \text{ cm}^{-2} \text{ s}^{-1} \text{ sr}^{-1} \text{ MeV}^{-1}$  at E = 0.6 MeV to  $33 \text{ cm}^{-2} \text{ s}^{-1} \text{ sr}^{-1} \text{ MeV}^{-1}$  at 8.0 MeV



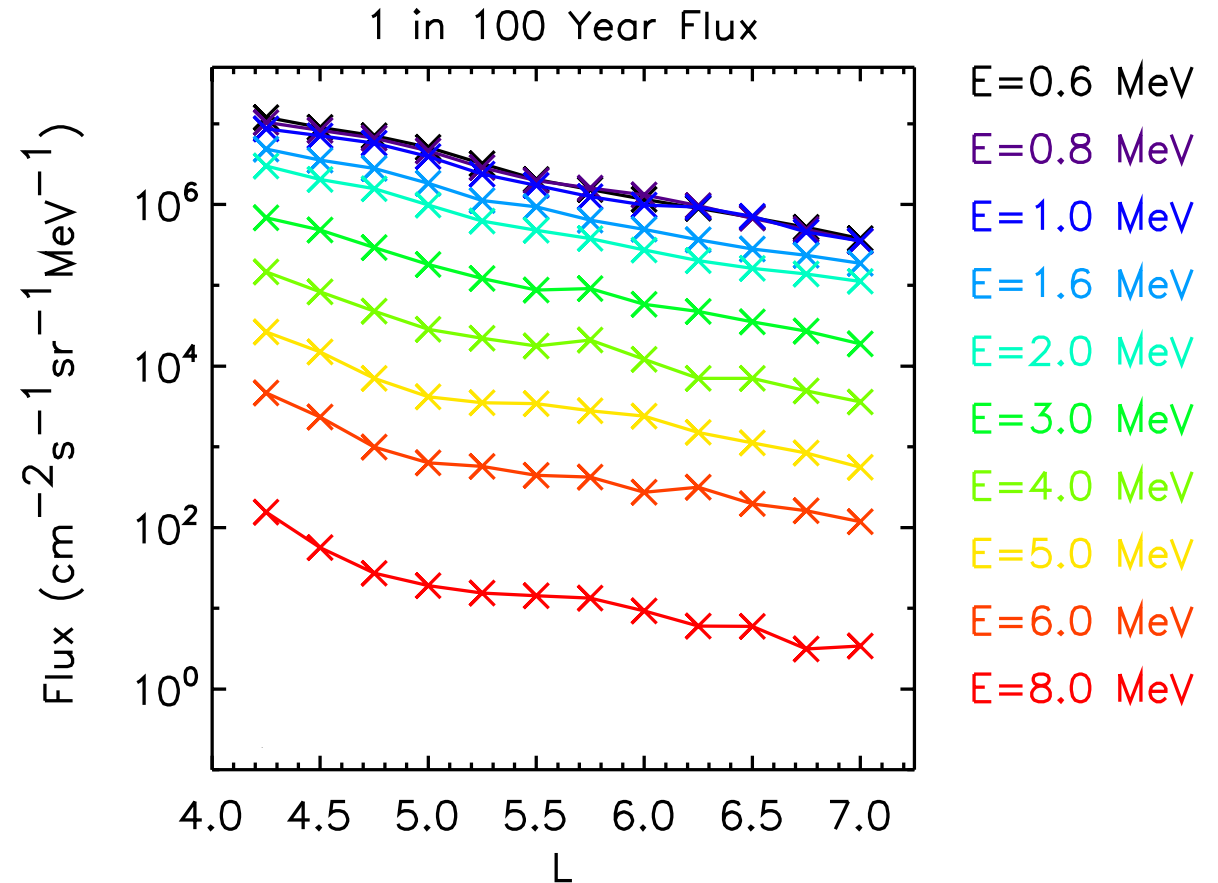
# 1 in 10 Year Fluxes as a function of L and Energy

- We can summarise the 1 in N year electron fluxes as a function of L for the different energies
- The 1 in 10 year flux at L = 4.5 ranges from  $8.2 \times 10^6 \text{ cm}^{-2} \text{ s}^{-1} \text{ sr}^{-1} \text{ MeV}^{-1}$  at E = 0.6 MeV to  $33 \text{ cm}^{-2} \text{ s}^{-1} \text{ sr}^{-1} \text{ MeV}^{-1}$  at 8.0 MeV
- Further out, at L = 6.5 the 1 in 10 year flux ranges from  $6.2 \times 10^5 \text{ cm}^{-2} \text{ s}^{-1} \text{ sr}^{-1} \text{ MeV}^{-1}$  at E = 0.6 MeV to  $0.47 \text{ cm}^{-2} \text{ s}^{-1} \text{ sr}^{-1} \text{ MeV}^{-1}$  at 8.0 MeV



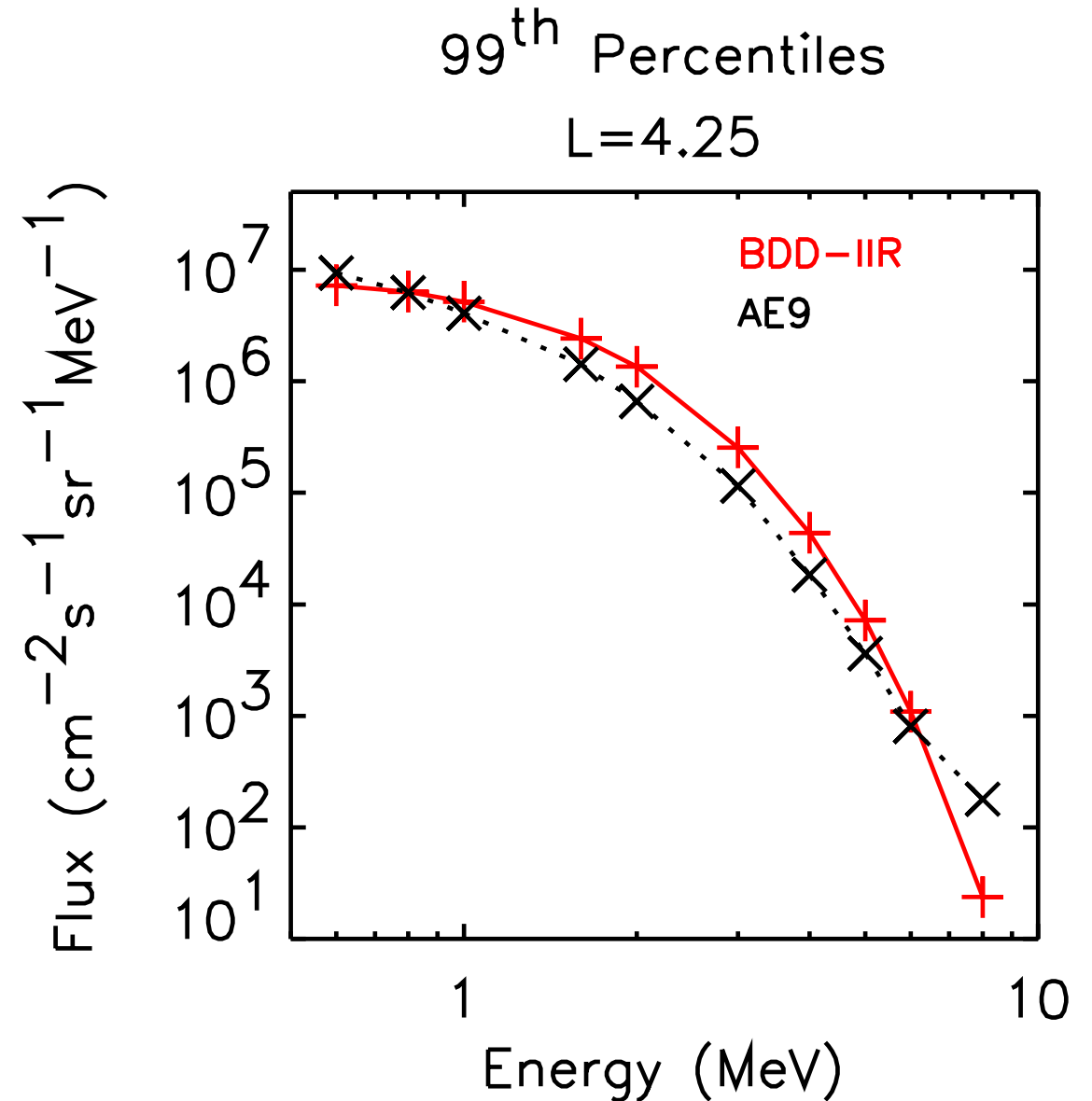
# 1 in 100 Year Fluxes as a function of L and Energy

- This figure shows the 1 in 100 year electron flux as a function of L for the different energies
- The 1 in 100 year fluxes are typically up to a factor of 2 to 10 times larger with the largest differences being at the higher L shells



# Comparison with the IRENE AE9 Radiation Environment Model

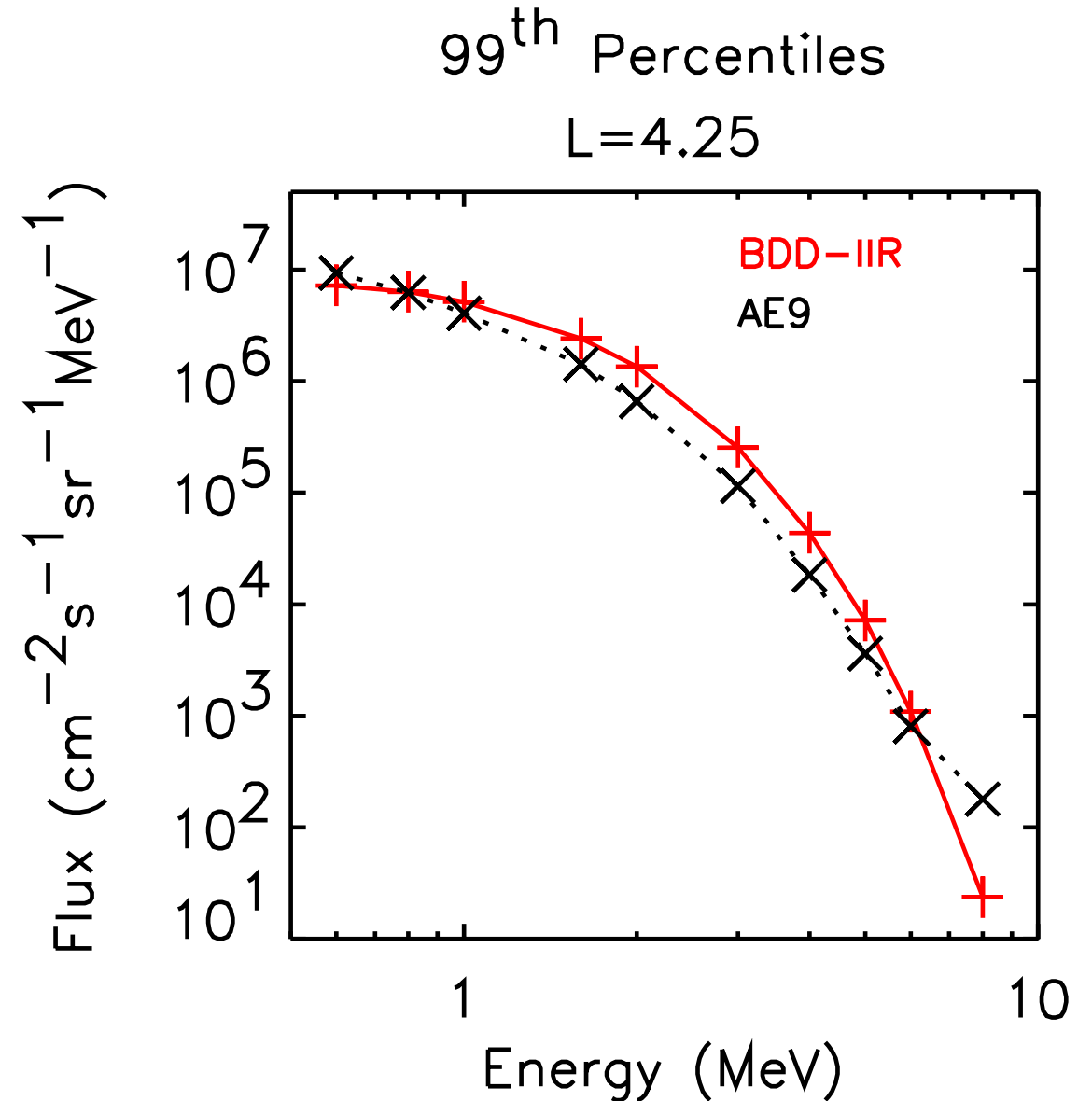
- It is interesting to compare the 99<sup>th</sup> percentiles of the NS41 fluxes with AE9
- The results are largely in extremely good agreement over the energy range 0.6 – 6.0 MeV
- The 99<sup>th</sup> percentile fluxes are about an order of magnitude less than AE9 at 8.0 MeV





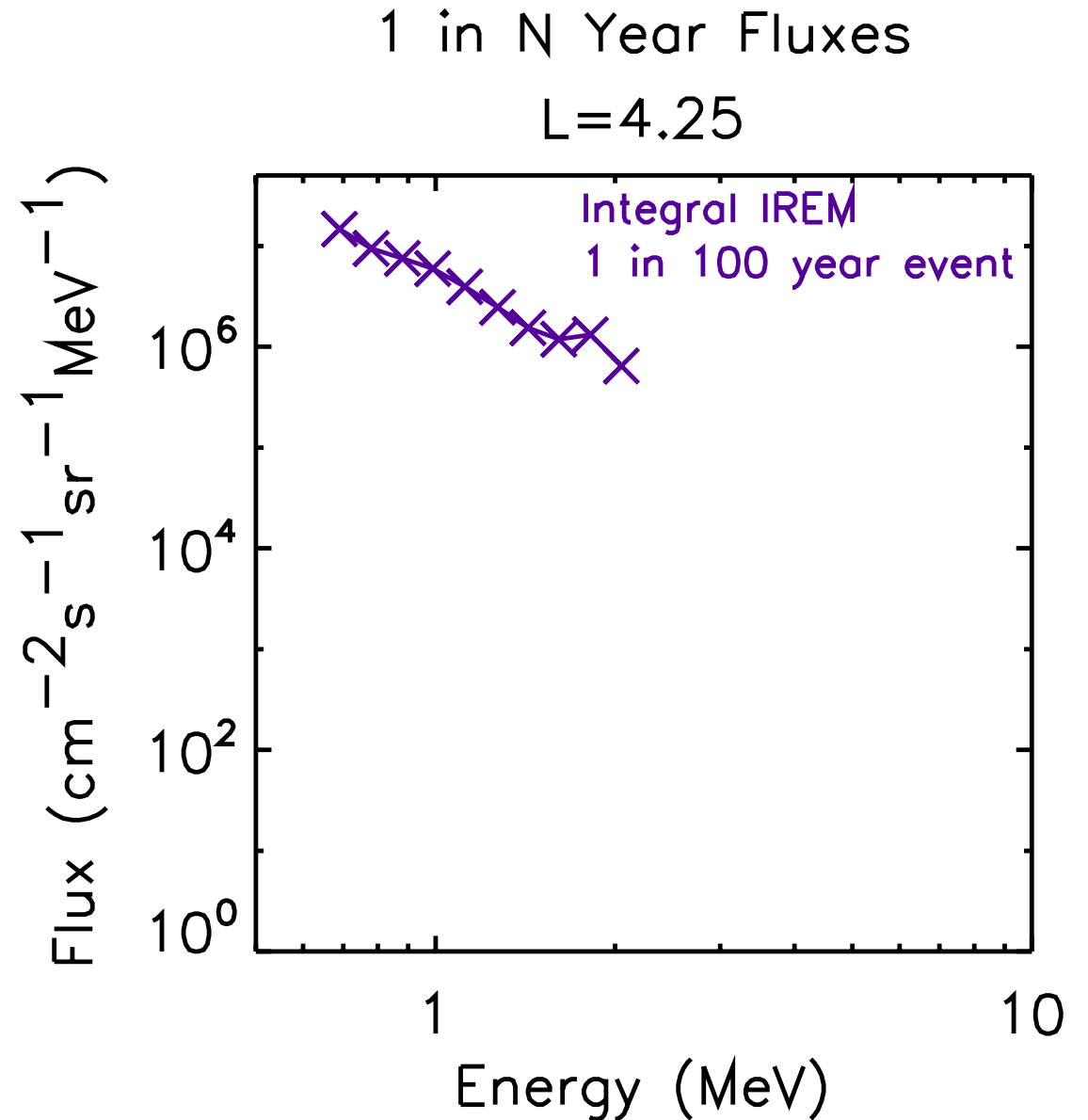
# Comparison with the IRENE AE9 Radiation Environment Model

- It is interesting to compare the 99<sup>th</sup> percentiles of the NS41 fluxes with AE9
- The results are largely in extremely good agreement over the energy range 0.6 – 6.0 MeV
- This could be due to background counting issues in the data used to construct AE9, especially as the gradient in the AE9 fluxes becomes less steep around 6.0 MeV



# Comparison with Integral IREM Results

- In 2017, we conducted an extreme value analysis using ~ 14 years of data from the Radiation Environment Monitor on board the Integral spacecraft (Meredith *et al.*, 2017)
- We can compare these findings with the new results from the NS41 BDD-IIR instrument

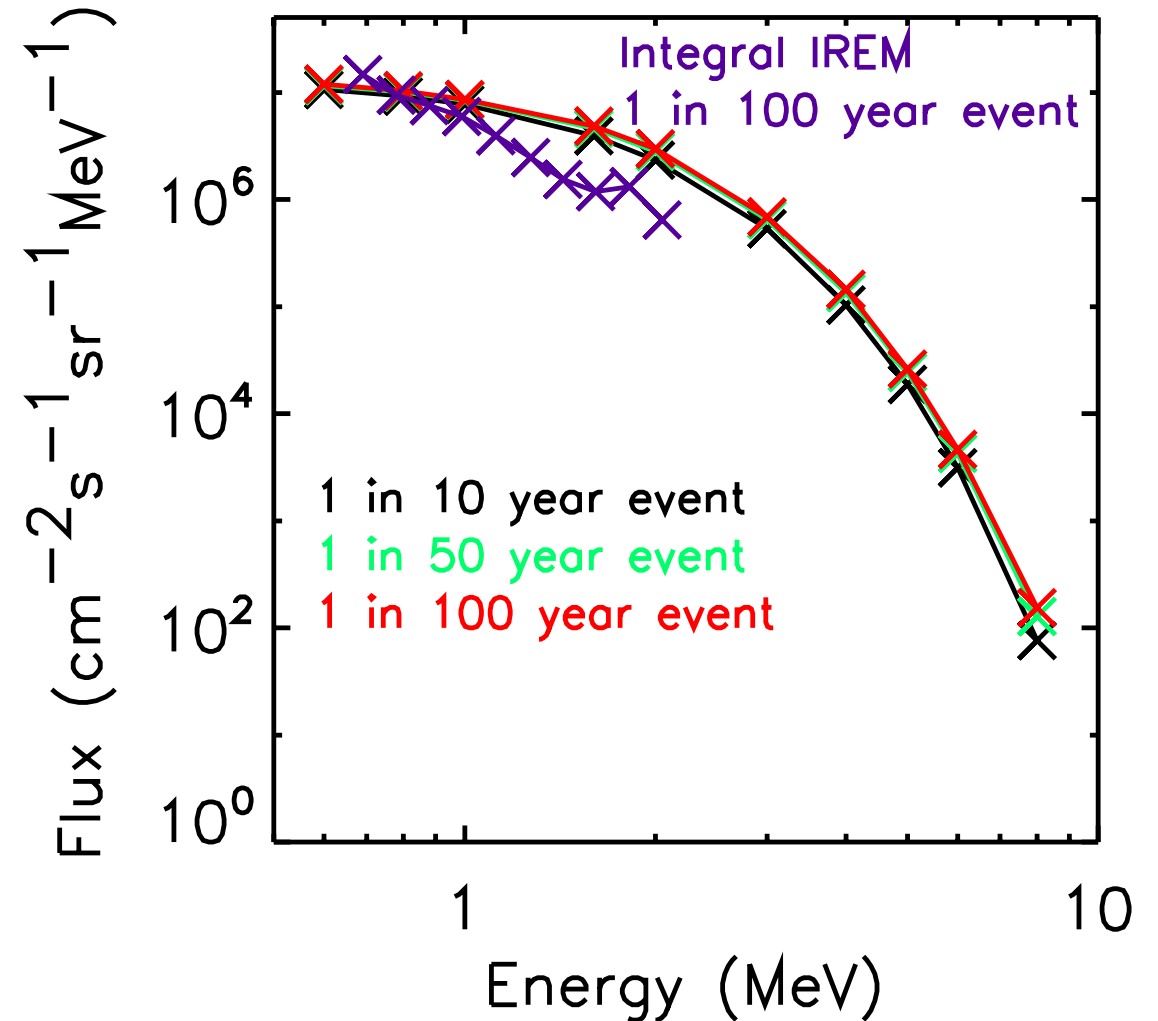


# Comparison with Integral IREM Results

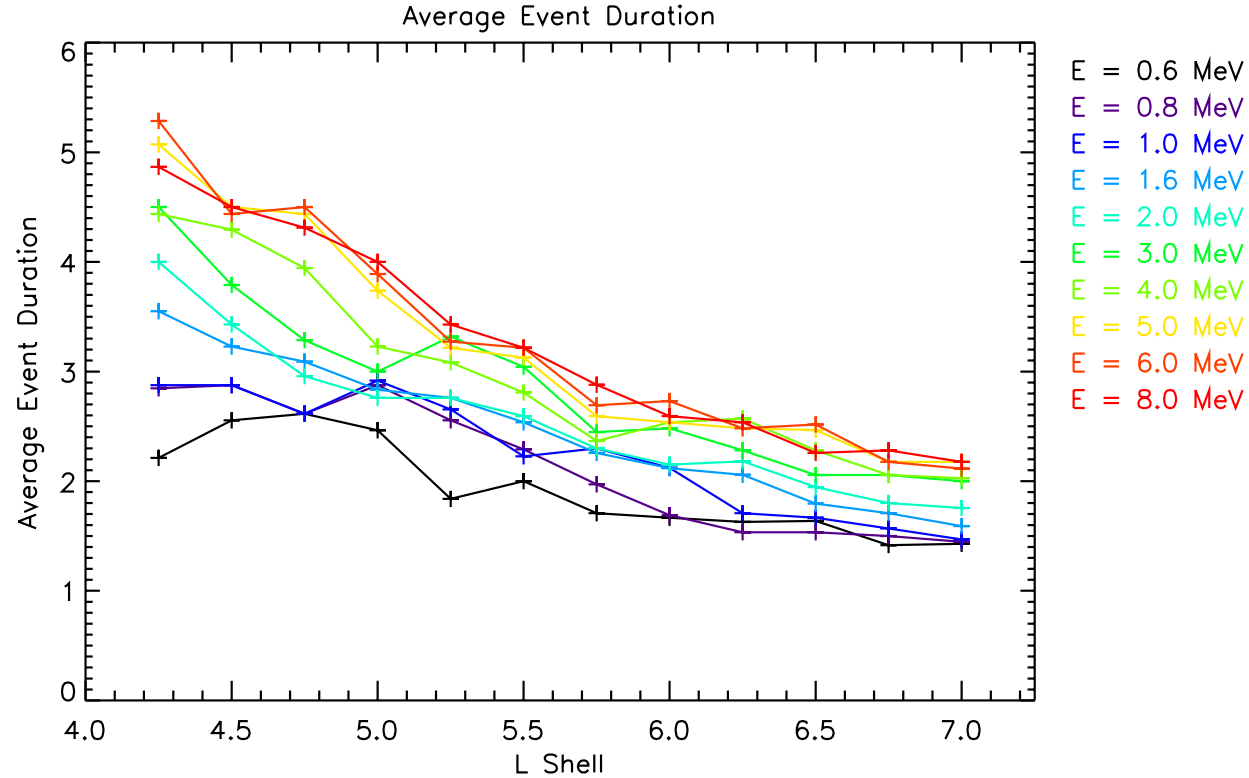
1 in N Year Fluxes

L=4.25

- The results are in good agreement at 0.8 and 1.0 MeV, but the Integral results are about a factor of 5 lower at 1.6 and ~ 2 MeV

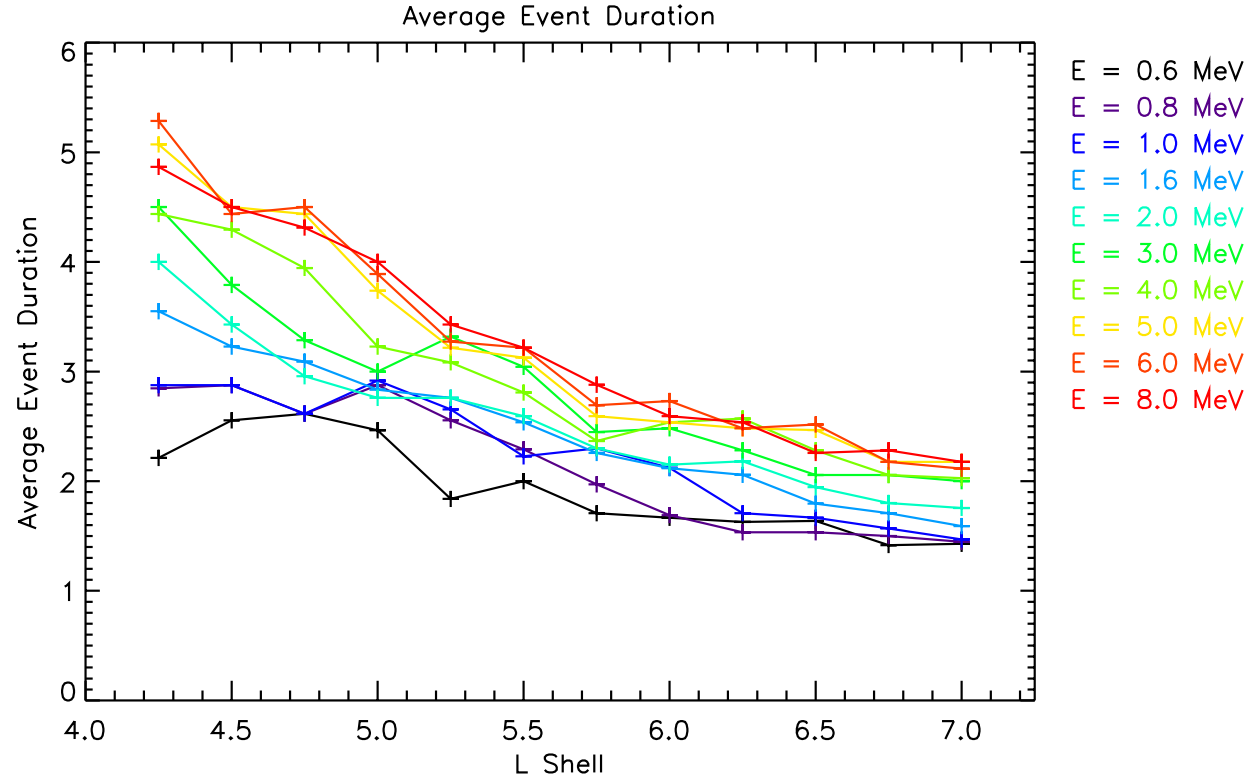


# Average Event Duration



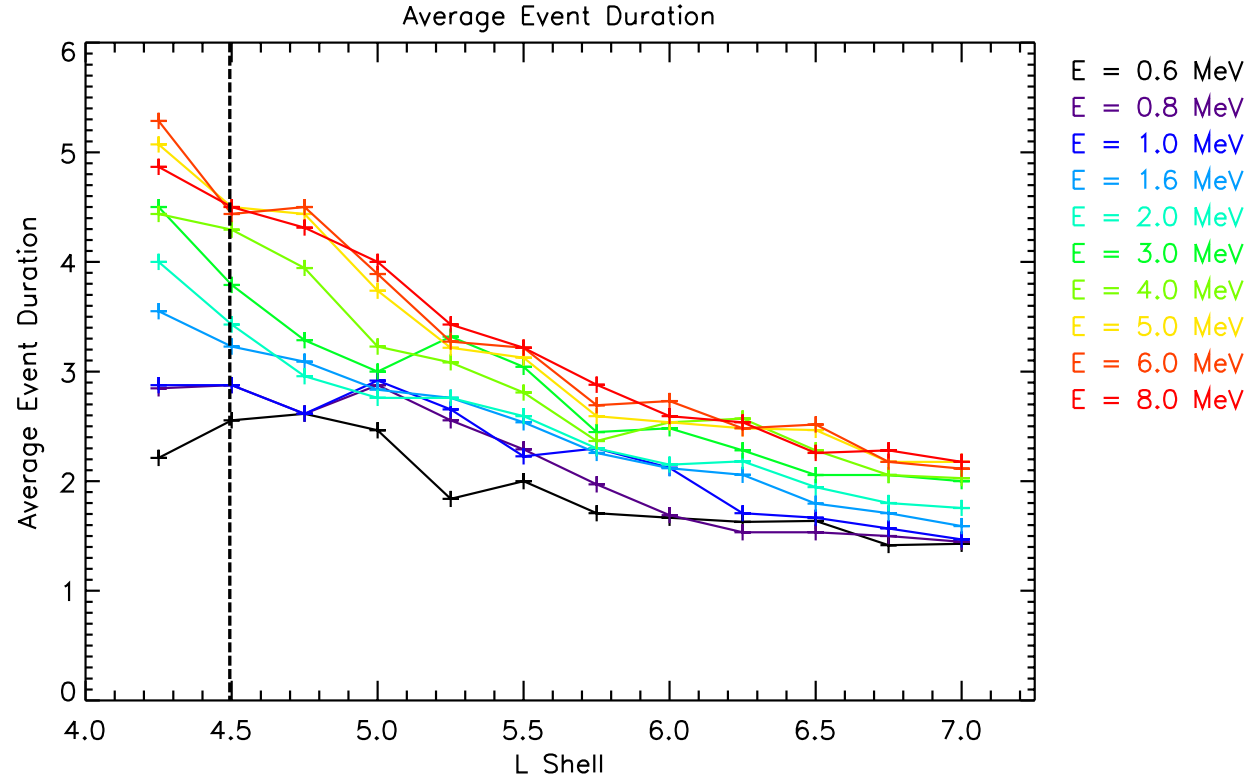
- This figure shows the average time the flux exceeds the 1% exceedance level for each of the cluster maxima for each energy as a function of L

# Average Event Duration



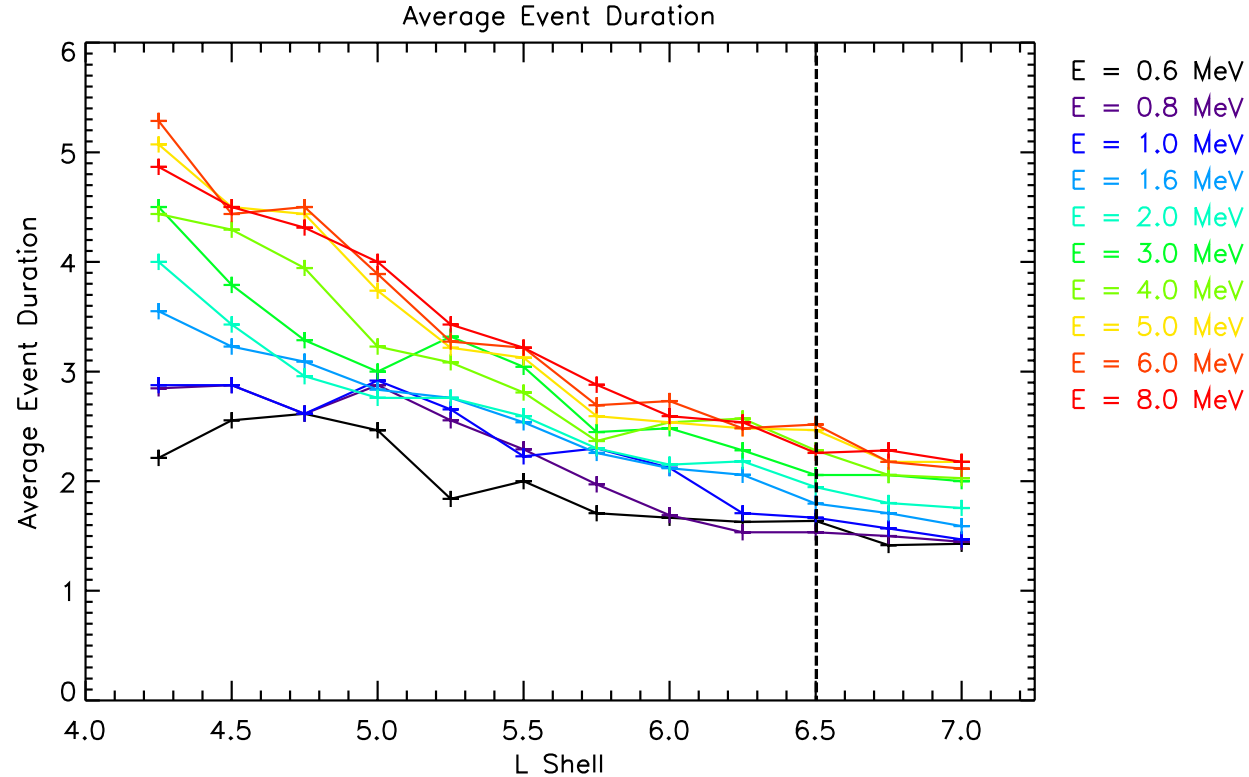
- This figure shows the average time the flux exceeds the 1% exceedance level for each of the cluster maxima for each energy as a function of L
- The average event duration increases with increasing energy and decreasing L

# Average Event Duration



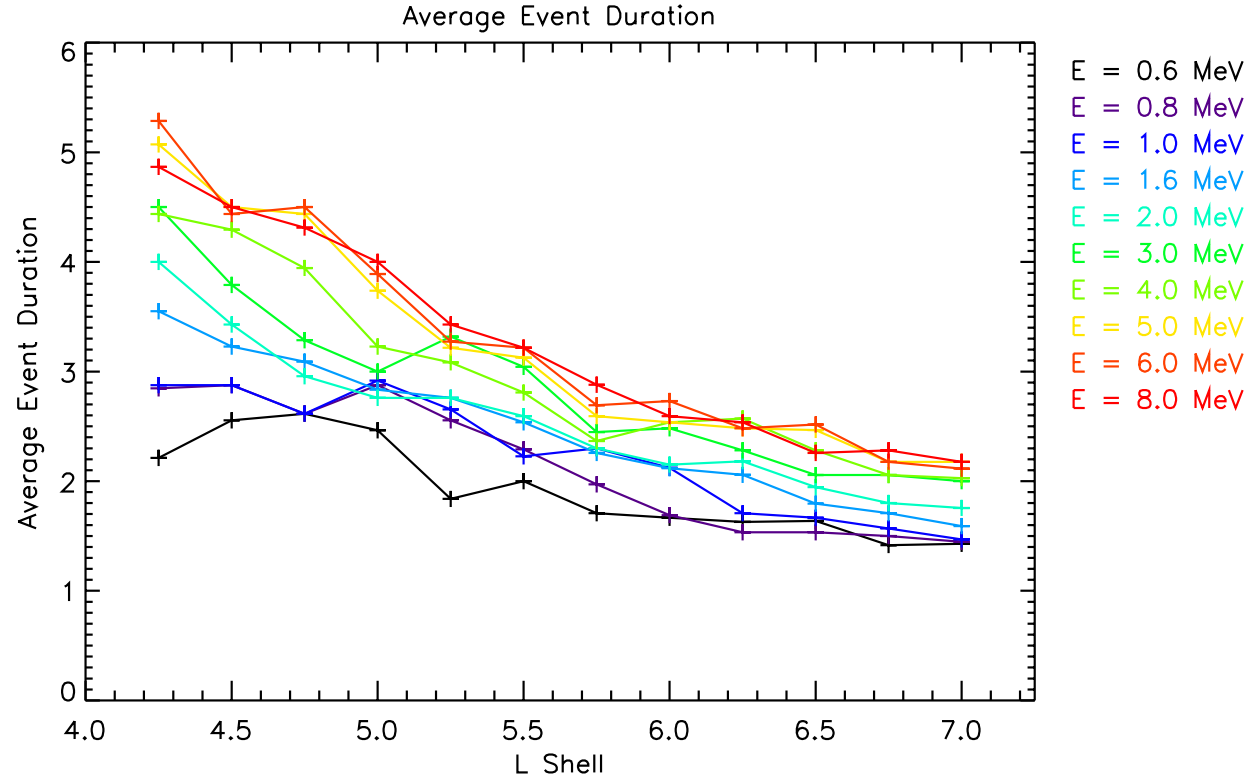
- Specifically, at L = 4.5, the average event duration increases from 2.5 days at E = 0.6 MeV to 4.4 days at the highest energies

# Average Event Duration



- Specifically, at  $L = 4.5$ , the average event duration increases from 2.5 days at  $E = 0.6$  MeV to 4.4 days at the highest energies
- Further out at  $L = 6.5$  we see the same trend, but the average duration is smaller ranging from 1.4 days at  $E = 0.6$  MeV to 2.5 days at  $E = 8.0$  MeV

# Average Event Duration

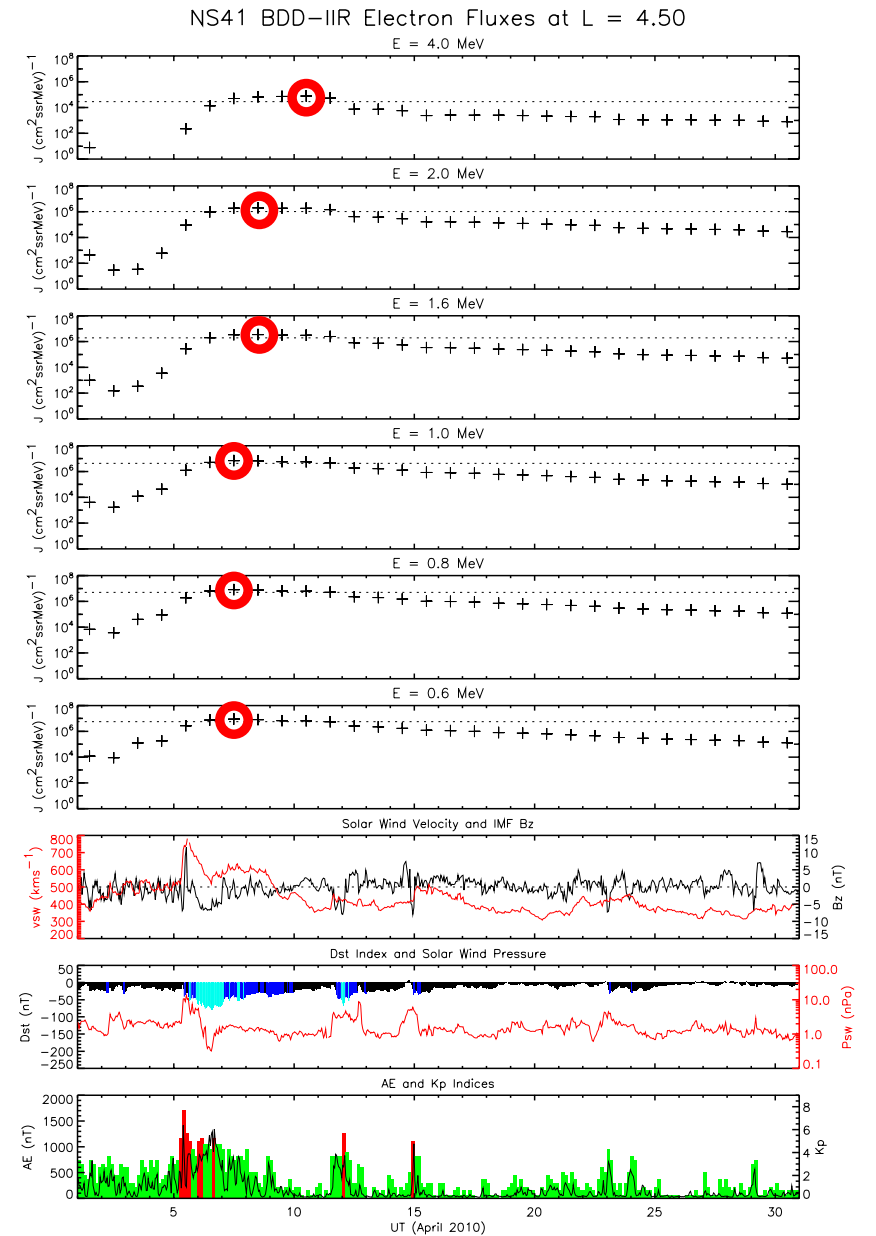


- Although we are not fitting timescales the data indicate that, over the range of energies and L samples, the timescale for loss is generally smaller at lower energies and higher L



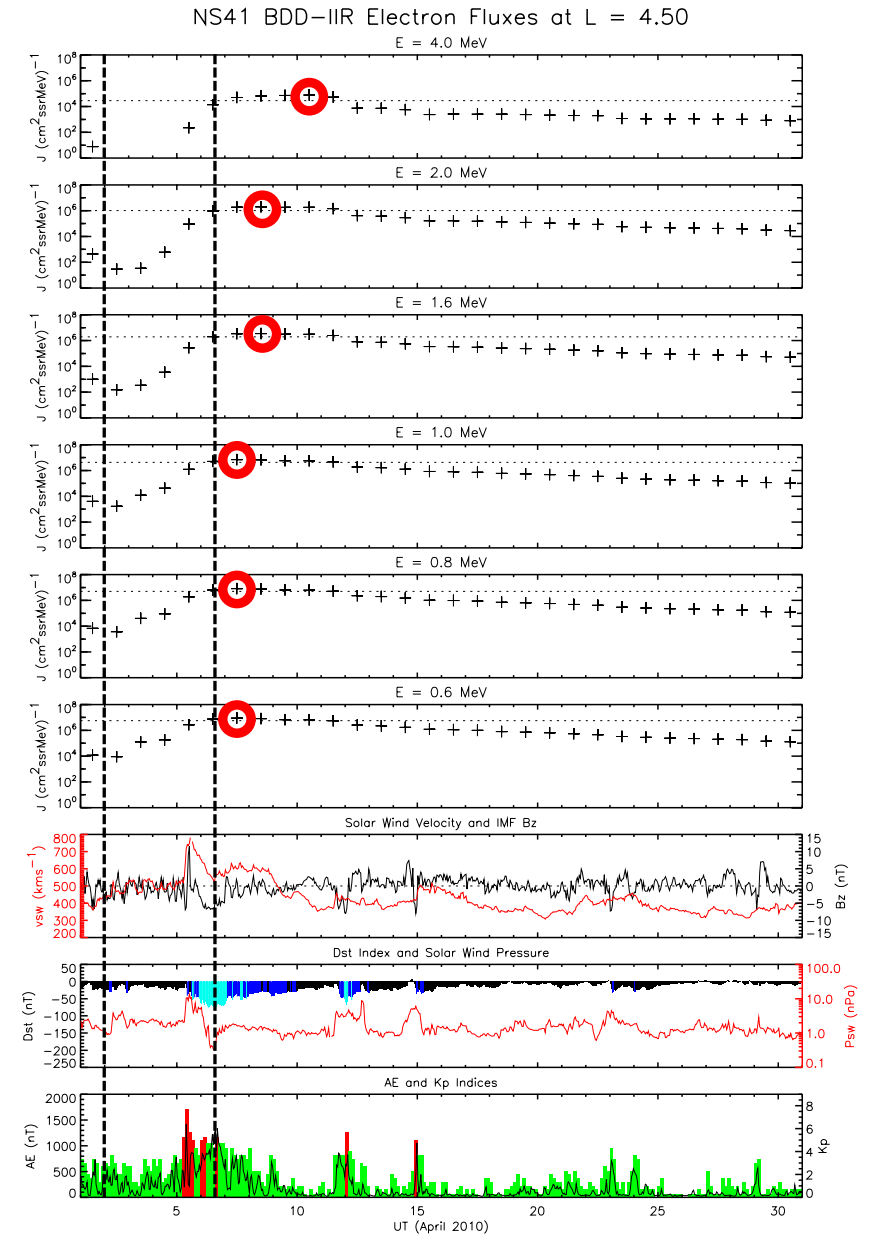
# Largest Event

- Some of the largest daily average fluxes encountered during the entire mission were observed during the 6 April 2010 geomagnetic storm
- This was a relatively moderate geomagnetic storm with a minimum Dst of -81 nT on 6 April



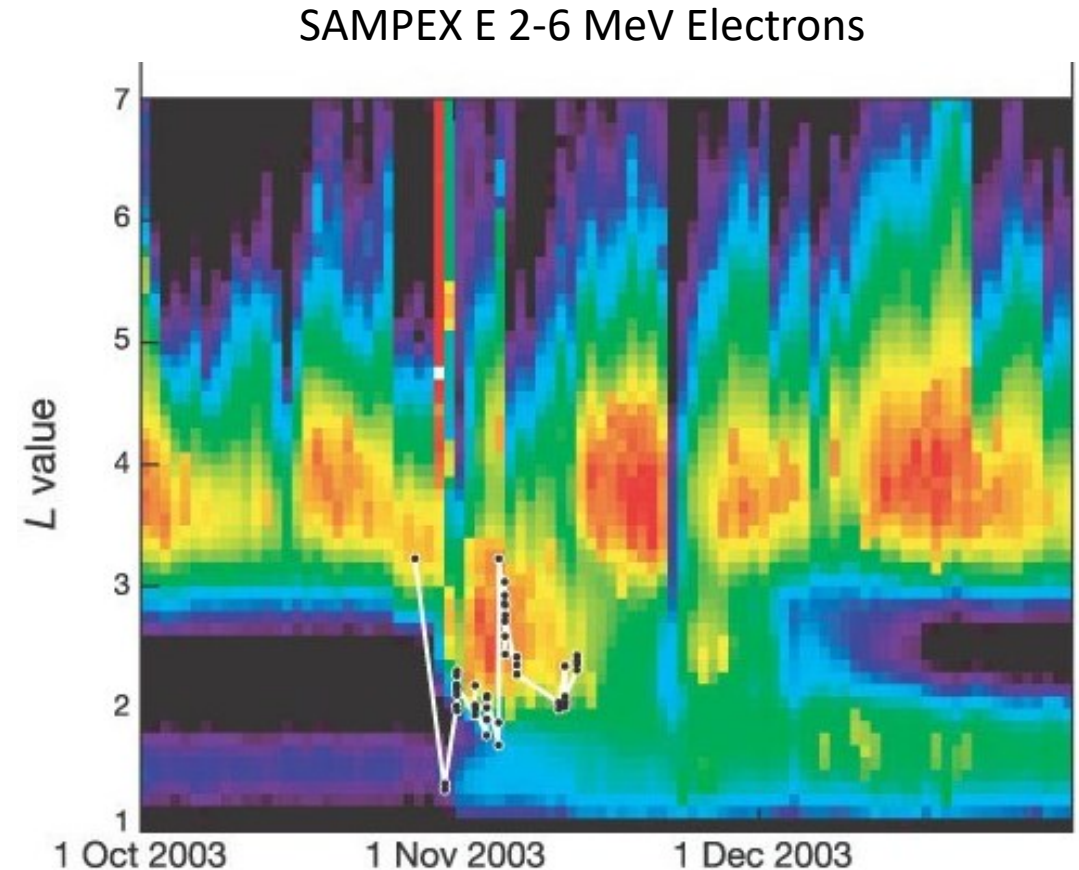
# Largest Event

- Some of the largest daily average fluxes encountered during the entire mission were observed during the 6 April 2010 geomagnetic storm
- This was a relatively moderate geomagnetic storm with a minimum Dst of -81 nT on 6 April
- Interestingly the relativistic electron fluxes had started to rise from 2 April, prior to the arrival of the storm due to a period of IMF Bz fluctuating about 0 nT and enhanced geomagnetic activity as monitored by AE



# Halloween Storm

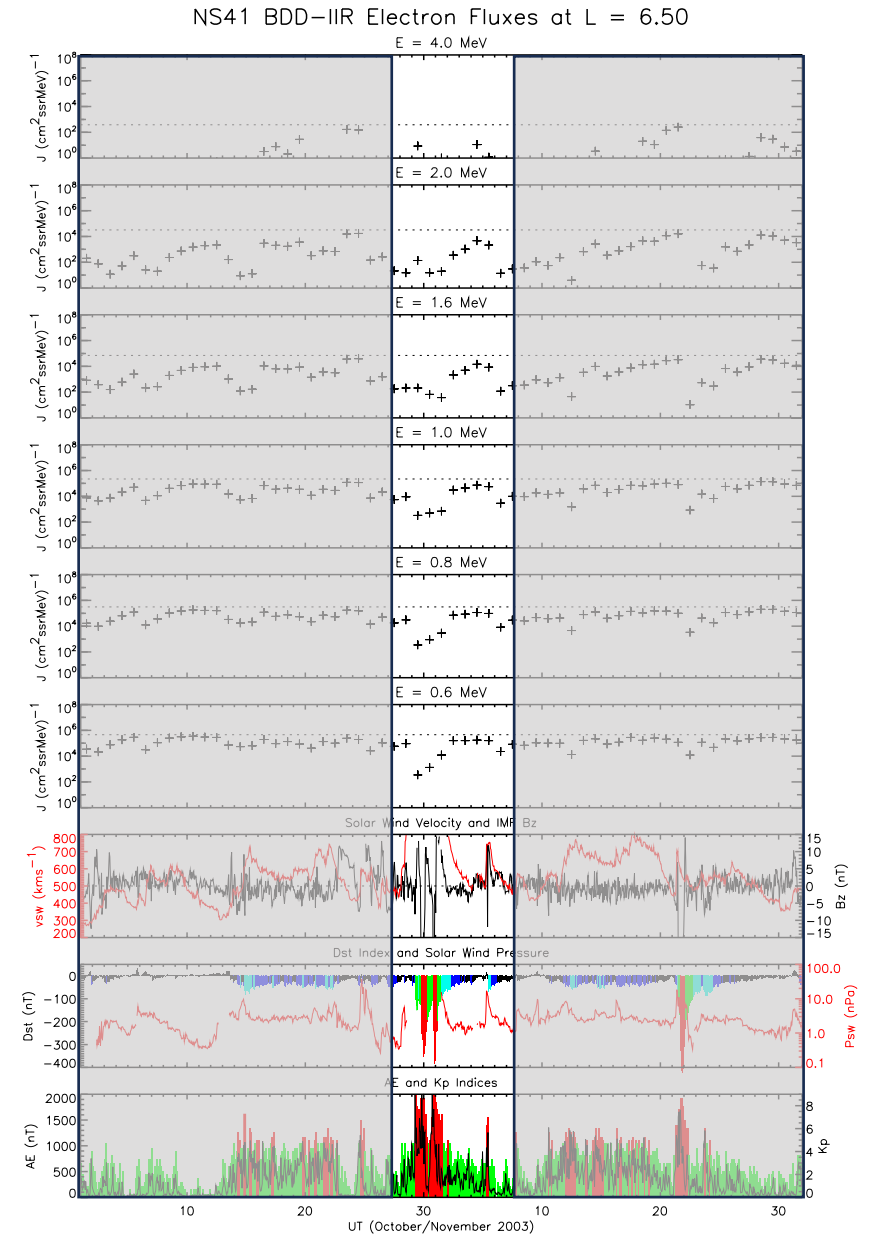
- One of the largest geomagnetic storms of the last 20 years was the Halloween storm in 2003, with a minimum Dst of -383 nT on 30<sup>th</sup> October
- Following the storm a new outer radiation belt formed at low L, peaking in the slot region below  $L = 3.0$



Baker et al., Nature, 2004

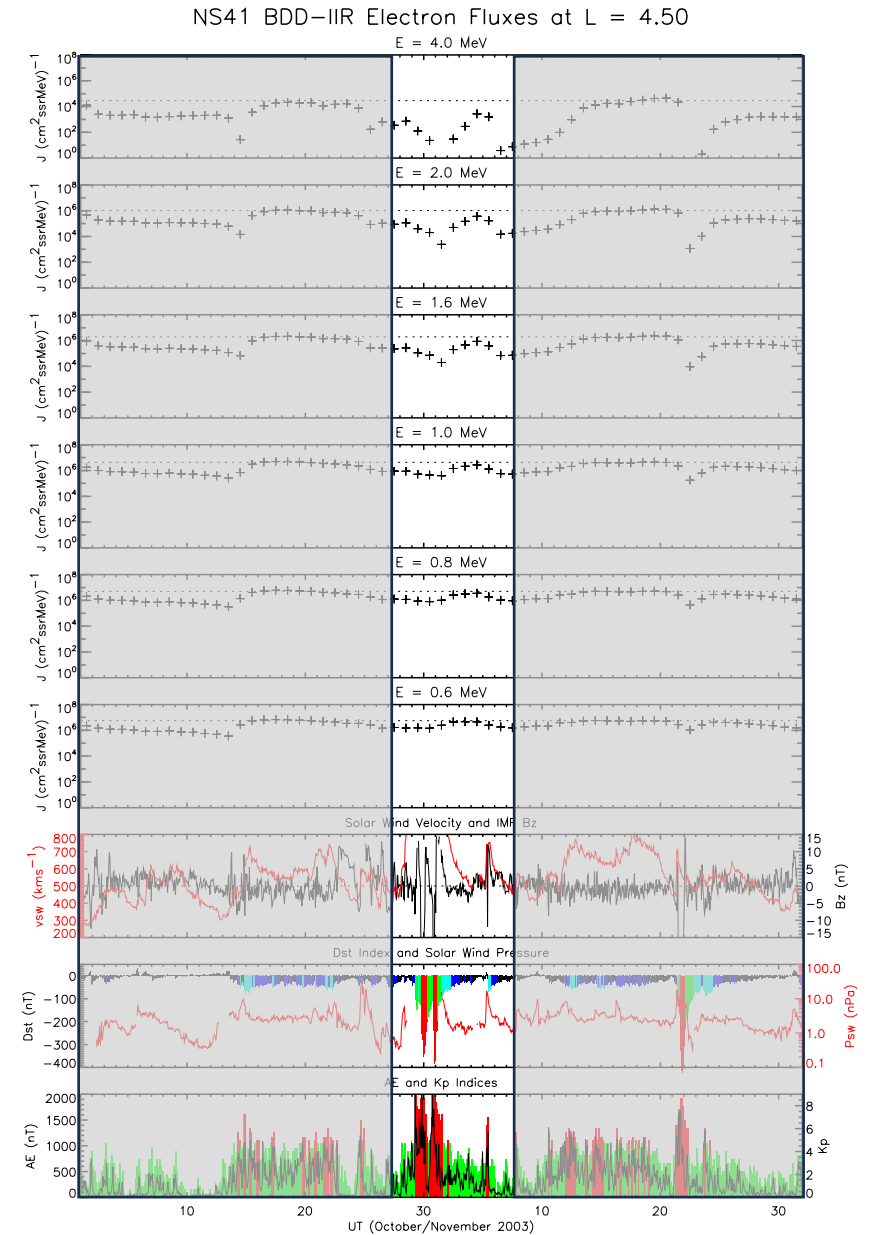
# Halloween Storm

- This storm was not associated with large fluxes of relativistic electrons as observed by NS41, either towards the outer edge of the outer radiation belt at L = 6.5



# Halloween Storm

- This storm was not associated with large fluxes of relativistic electrons as observed by NS41, either towards the outer edge of the outer radiation belt at  $L = 6.5$  or at the heart of the outer radiation belt at  $L = 4.5$



# Preliminary Storm Study

- These results suggests that modest storms may pose more of a risk to satellites in GPS orbit than the largest storms that are more typically associated with extreme space weather
- To examine this finding in more detail we looked at the top 50  $E = 2.0$  MeV flux events at  $L = 4.5$  and  $6.5$  and compared them with the largest fluxes associated with the top 15 strongest storms

# Storm Categories

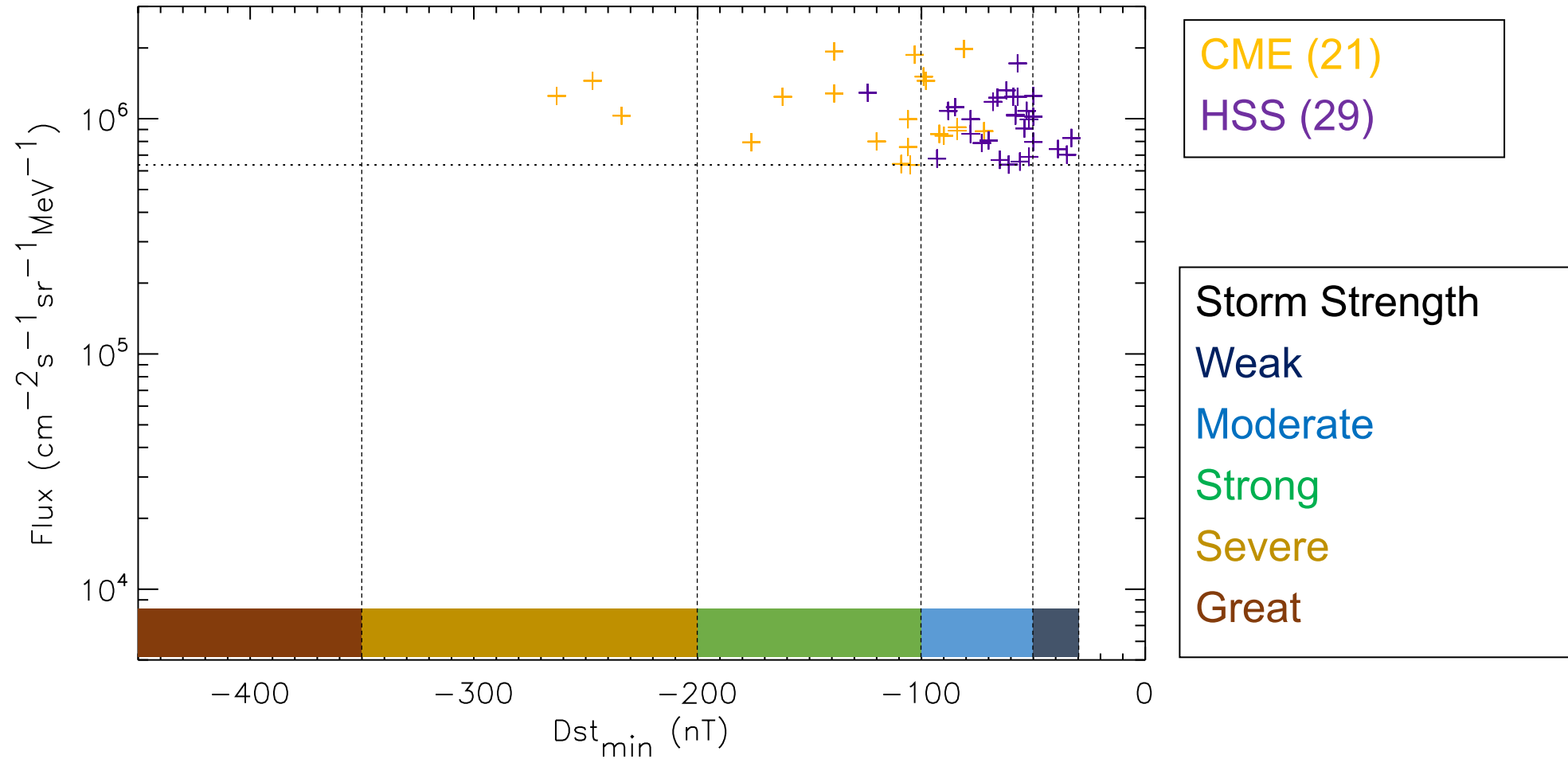
- We classify the storm strength by the minimum value of the Dst index associated with the storm, defined by Loewe and Prolss (1997) as follows:
  - **Weak** ( $-50 < \text{Dst}_{\min} < -30$  nT)
  - **Moderate** ( $-100 < \text{Dst}_{\min} < -50$  nT)
  - **Strong** ( $-200 < \text{Dst}_{\min} < -100$  nT)
  - **Severe** ( $-350 < \text{Dst}_{\min} < -200$ )
  - **Great** ( $\text{Dst}_{\min} < -350$  nT)

# Storm Categories

- We classify the storm strength by the minimum value of the Dst index associated with the storm, defined by Loewe and Prolss (1997) as follows:
  - **Weak** ( $-50 < \text{Dst}_{\min} < -30$  nT)
  - **Moderate** ( $-100 < \text{Dst}_{\min} < -50$  nT)
  - **Strong** ( $-200 < \text{Dst}_{\min} < -100$  nT)
  - **Severe** ( $-350 < \text{Dst}_{\min} < -200$ )
  - **Great** ( $\text{Dst}_{\min} < -350$  nT)
- We further split the storms into two groups:
  - **Coronal Mass Ejections (CME)**
  - **High Speed Solar Wind Streams (HSS)**

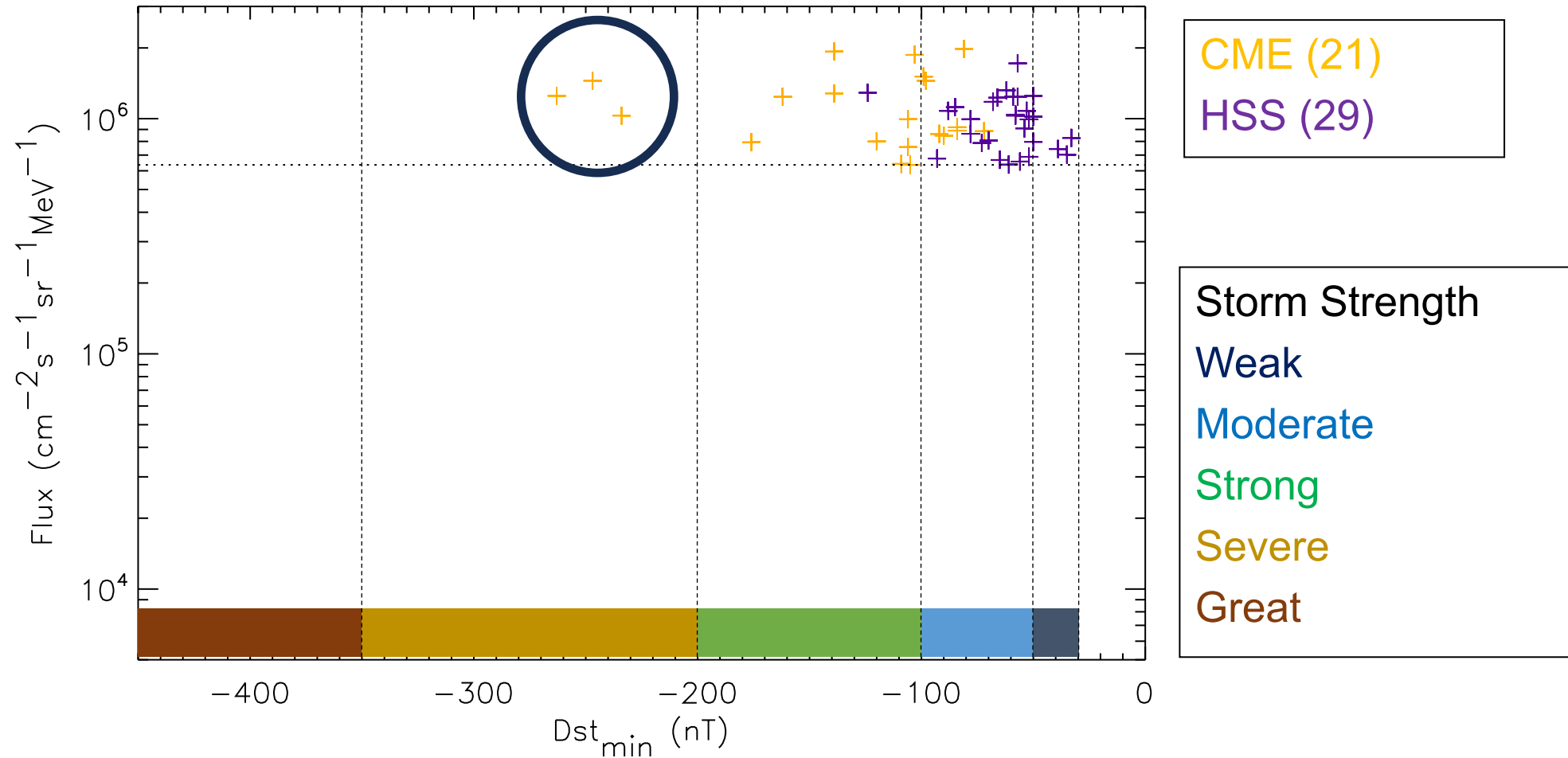


# Top 50 E = 2.0 MeV Flux Events at L = 4.5



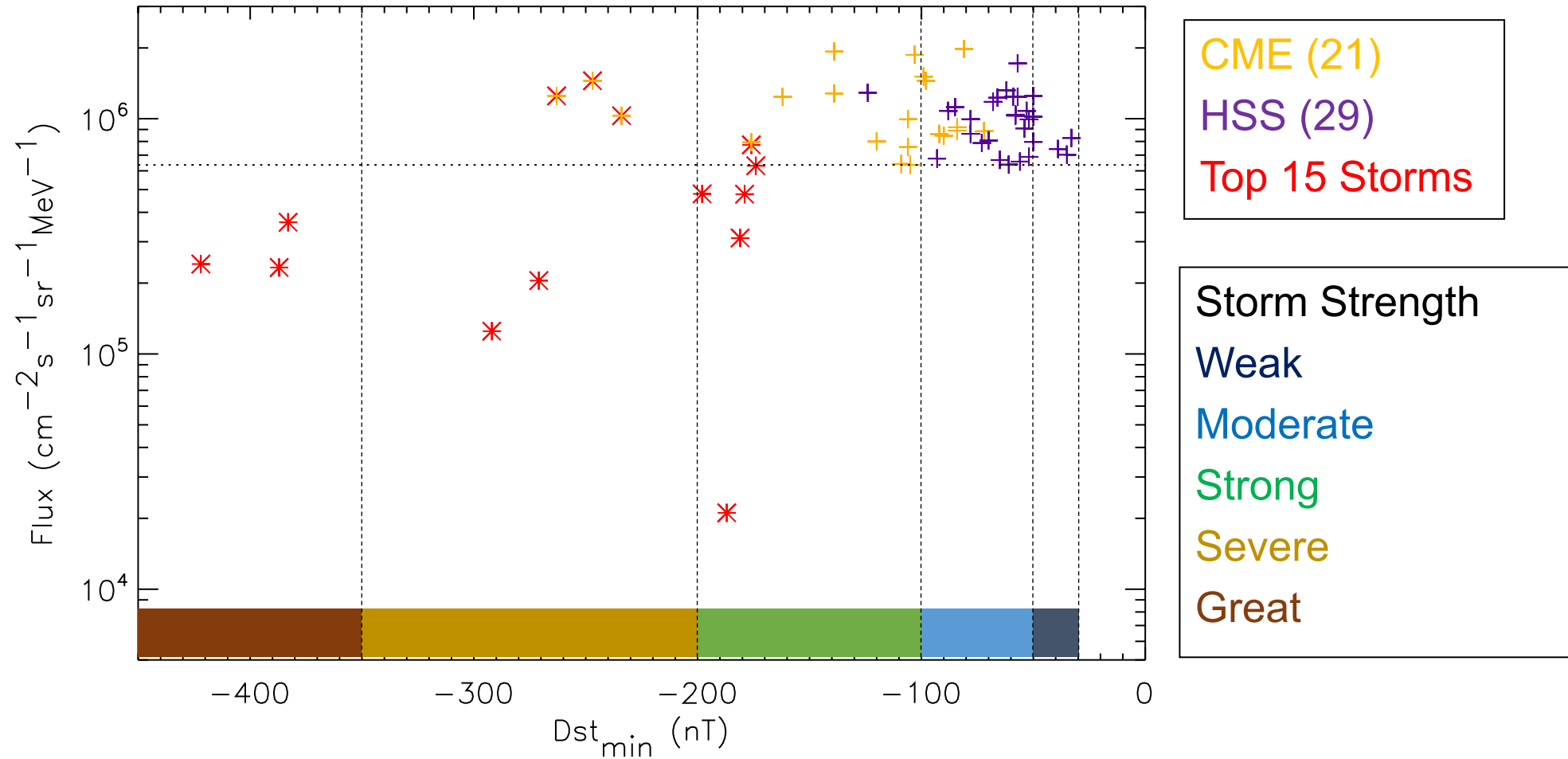
- At L = 4.5 the majority of the largest flux enhancements are associated with weak and moderate geomagnetic storms

# Top 50 E = 2.0 MeV Flux Events at L = 4.5



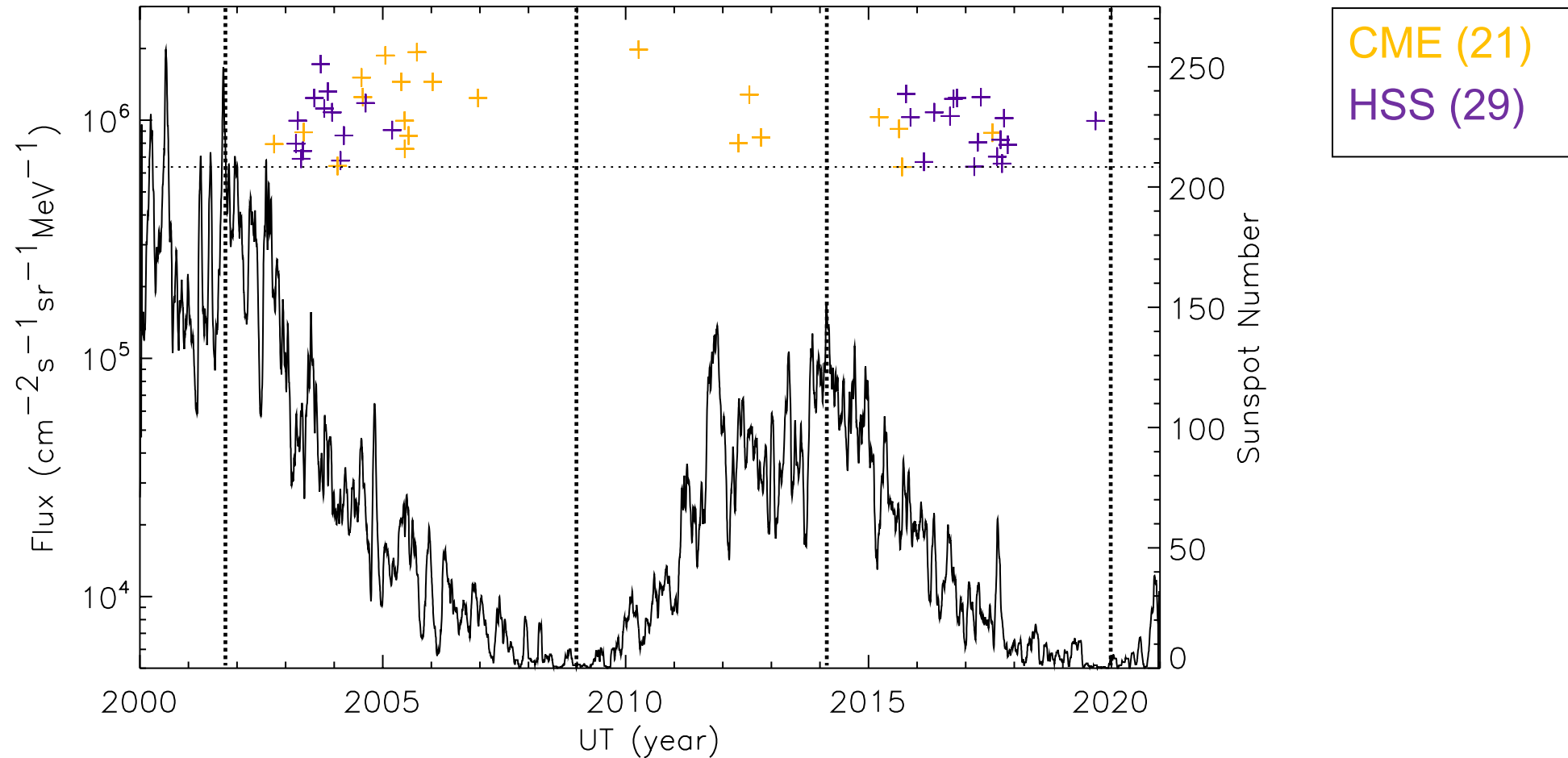
- At L = 4.5 the majority of the largest flux enhancements are associated with weak and moderate geomagnetic storms
- While it is possible to have a large flux associated with a severe storm, the latter is not a requirement for a large flux event

# Top 50 E = 2.0 MeV Flux Events at L = 4.5



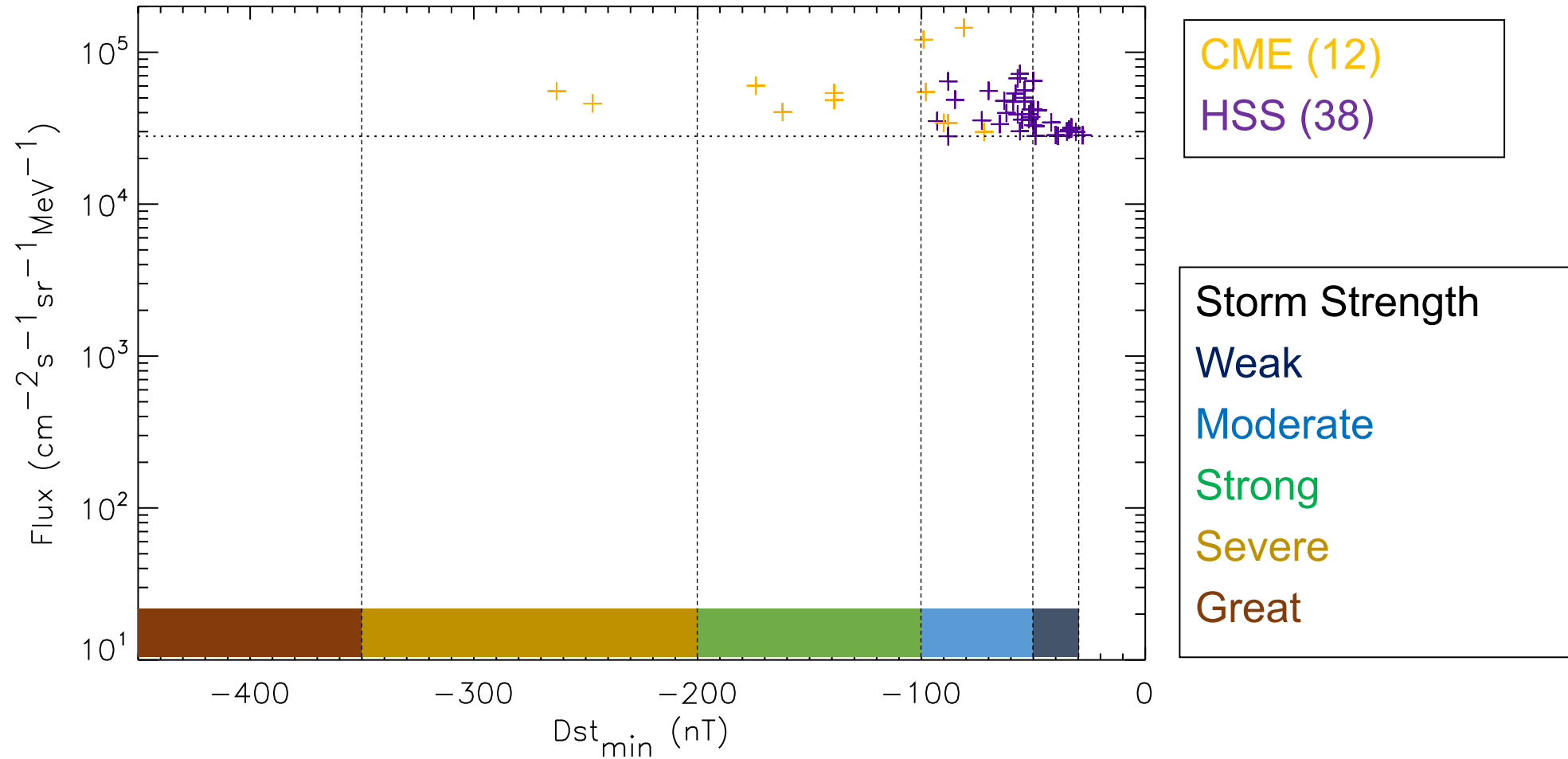
- At L = 4.5 the majority of the largest storms do not lead to significant flux events

# Top 50 E = 2.0 MeV Flux Events at L = 4.5



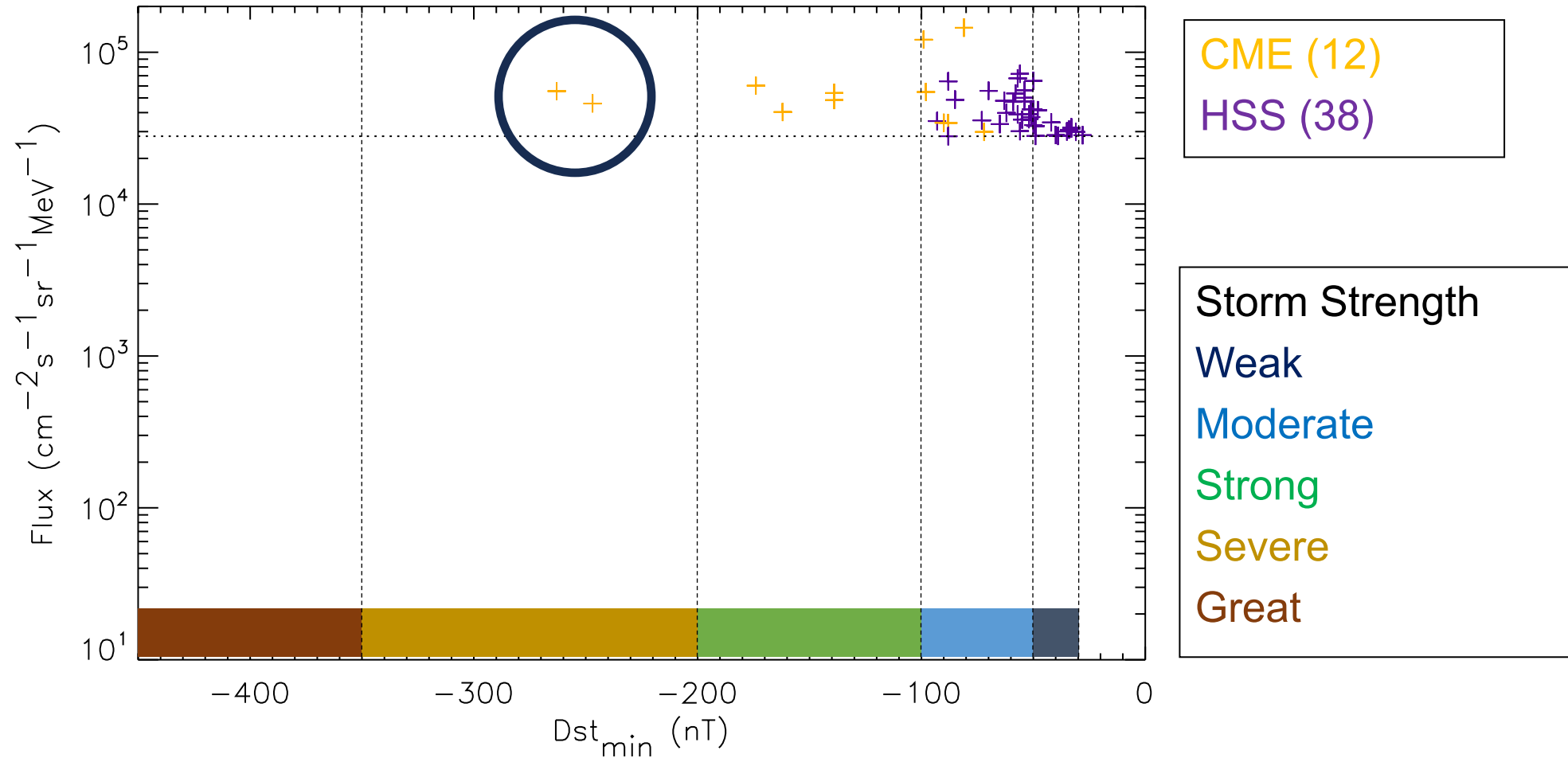
- At L = 4.5 the majority of the largest fluxes are seen during the declining phases of solar cycles 23 and 24

# Top 50 E = 2.0 MeV Flux Events at L = 6.5



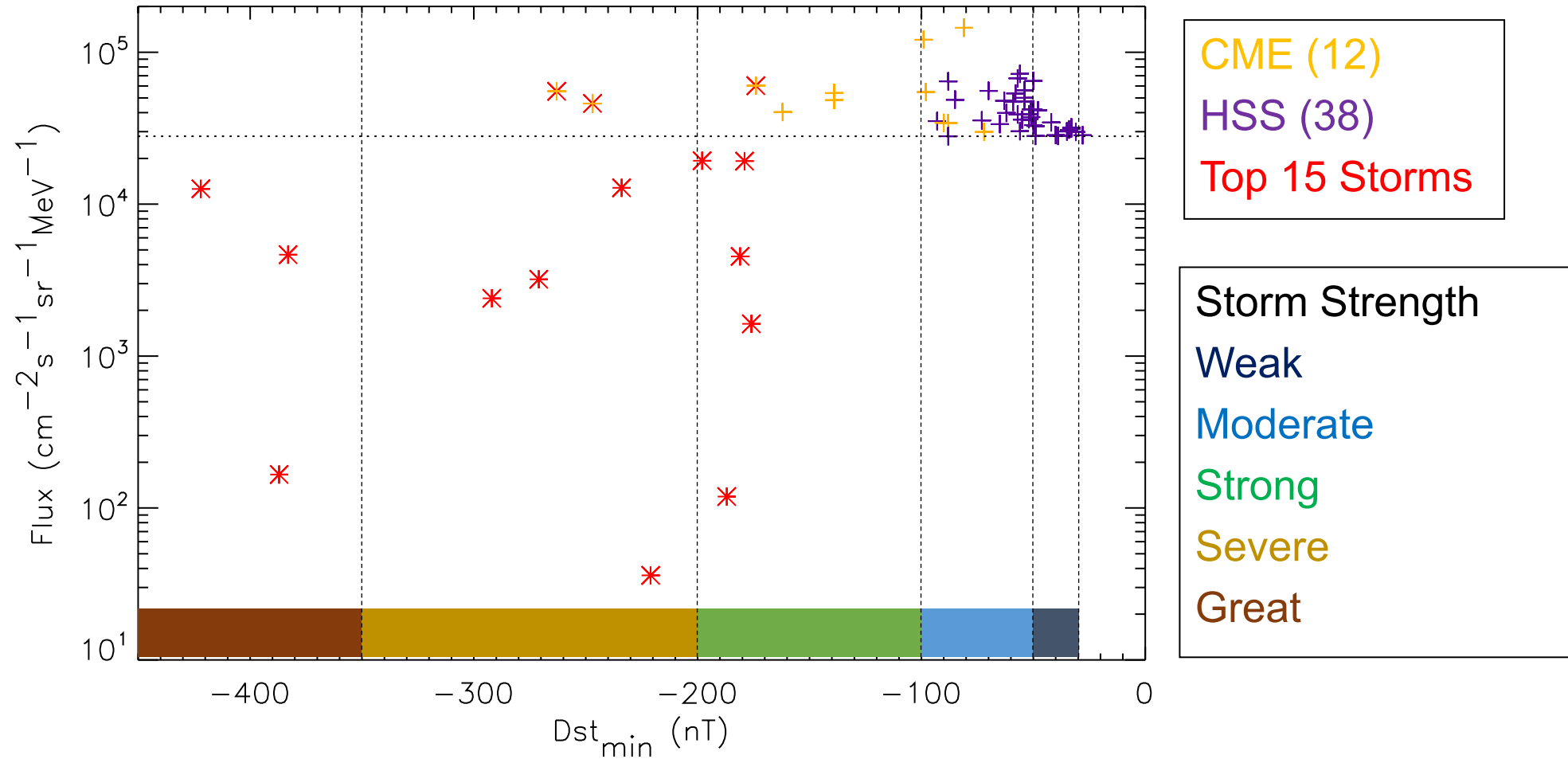
- At L = 6.5 the majority of the largest flux enhancements are also associated with weak and moderate geomagnetic storms

# Top 50 E = 2.0 MeV Flux Events at L = 6.5



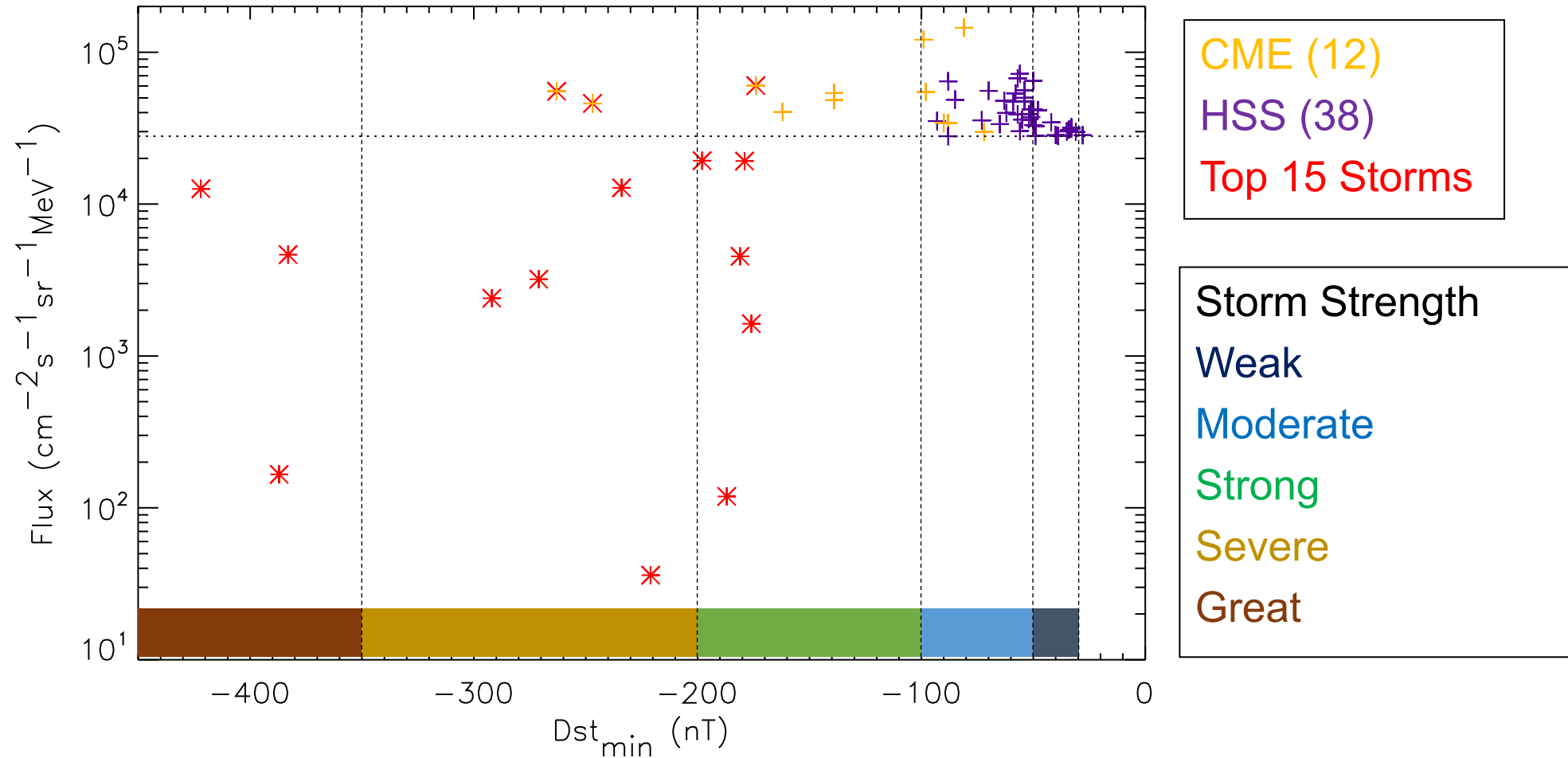
- At L = 6.5 the majority of the largest flux enhancements are also associated with weak and moderate geomagnetic storms
- Again, while it is possible to have a large flux associated with a severe storm, the latter is not a requirement for a large flux event

# Top 50 E = 2.0 MeV Flux Events at L = 6.5



- At L = 6.5 the majority of the largest storms do not lead to significant flux events

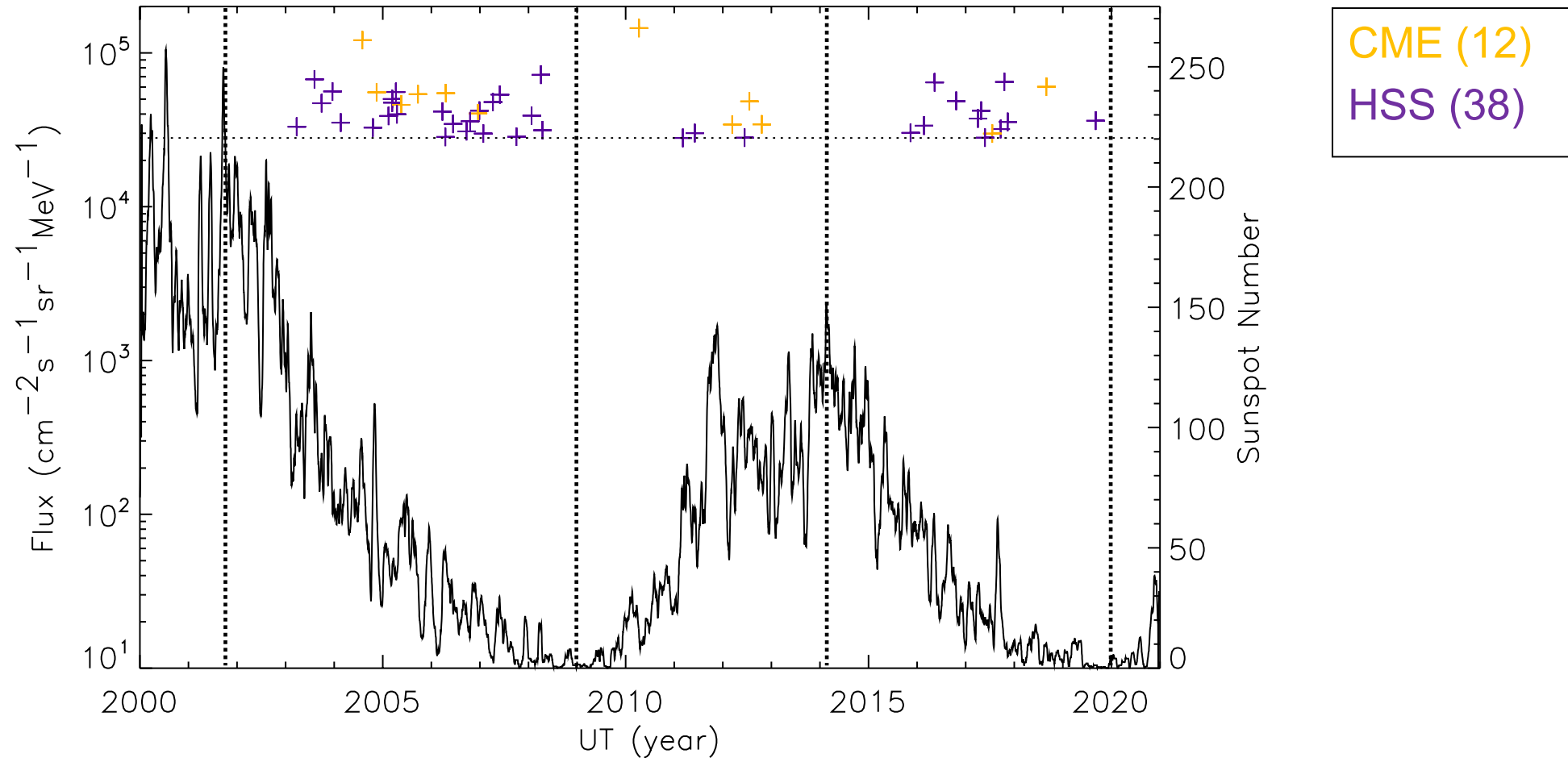
# Top 50 E = 2.0 MeV Flux Events at L = 6.5



- At L = 6.5 the majority of the largest storms do not lead to significant flux events
- *This study shows that the largest relativistic electron fluxes in GPS orbit are not related to the most extreme storms as monitored by the Dst index*



# Top 50 E = 2.0 MeV Flux Events at L = 6.5



- At L = 6.5 the majority of the largest flux events are seen during the declining phases of solar cycles 23 and 24

# Applications

- The 1 in 10 and 1 in 100 year flux levels as a function of energy and L serve as benchmarks
  - to compare against other extreme space weather events
  - to help assess the potential impact of an extreme event
  - to improve the resilience of future satellites
  - to help evaluate realistic disaster scenarios

# Conclusions

- The 1 in 10 year flux at  $L = 4.5$ , near the heart of the outer radiation belt, decreases with increasing energy ranging from  $8.2 \times 10^6 \text{ cm}^{-2} \text{ s}^{-1} \text{ sr}^{-1} \text{ MeV}^{-1}$  at  $E = 0.6 \text{ MeV}$  to  $33 \text{ cm}^{-2} \text{ s}^{-1} \text{ sr}^{-1} \text{ MeV}^{-1}$  at  $E = 8.0 \text{ MeV}$ . The 1 in 100 year event exhibits a similar trend and is a factor of 1.1 to 1.7 larger than the corresponding 1 in 10 year event.
- The 1 in 10 year flux at  $L = 6.5$ , on field lines which map to the vicinity of geostationary orbit, decrease with increasing energy ranging from  $6.2 \times 10^5 \text{ cm}^{-2} \text{ s}^{-1} \text{ sr}^{-1} \text{ MeV}^{-1}$  at  $E = 0.6 \text{ MeV}$  to  $0.47 \text{ cm}^{-2} \text{ s}^{-1} \text{ sr}^{-1}$  at  $E = 8.0 \text{ MeV}$ . The 1 in 100 year event exhibits a similar trend and is a factor of 1.1 to 12 times larger than the corresponding 1 in 10 year event.

# Acknowledgements

- We would like to acknowledge the skill and attention to detail of Timothy J. Wehner that enabled these measurements at Medium Earth Orbit
- We acknowledge Los Alamos National Laboratory for generating the BDD-IIR data products used in this study, and the National Oceanic and Atmospheric Administration's archive of the data files themselves
- The research leading to these results has received funding from the Natural Environment Research Council Grants NE/V00249X/1 (Sat-Risk) and NE/ R016038/1